Published for SISSA by Springer

Received: May 6, 2022
Revised: August 23, 2022
Accepted: October 3, 2022
Published: October 20, 2022

Leptonic cascade decays of a heavy Higgs boson through vectorlike leptons at the LHC

Radovan Dermisek,[a] **Junichiro Kawamura,**[b] **Enrico Lunghi,**[a] **Navin McGinnis**[c] **and Seodong Shin**[b,d]

[a] *Physics Department, Indiana University, Bloomington, IN 47405, U.S.A.*
[b] *Center for Theoretical Physics of the Universe, Institute for Basic Science, Daejeon 34126, Korea*
[c] *TRIUMF, 4004 Westbrook Mall, Vancouver, BC, Canada V6T 2A3*
[d] *Department of Physics, Jeounbuk National University, Jeonju, Jeonbuk 54896, Korea*

E-mail: dermisek@indiana.edu, jkawa@ibs.re.kr, elunghi@indiana.edu, nmcginnis@triumf.ca, sshin@jbnu.ac.kr

Abstract: We demonstrate the potential of fully leptonic cascade decays of a heavy neutral Higgs boson through vectorlike leptons as a simultaneous probe for extended Higgs sectors and extra matter particles at the LHC. The processes we explore are unique in that their event topologies lead to di-boson-like leptonic final states with a lepton pair which does not reconstruct the mass of a gauge boson. By recasting existing $2\ell + E_T^{\rm miss}$ and $3/4\ell$ searches channels using run2 data from the LHC we obtain *model independent* bounds on the masses of heavy scalars and vectorlike leptons and use these results to explore future prospects at the HL-LHC. Our results can be directly applied to any kind of new physics scenarios sharing the final states and the event topology. For concreteness, we apply our results to a benchmark scenario: a two Higgs doublet model type-II augmented with vectorlike leptons. Remarkably, even with current data the sensitivity of our analysis shows a reach for masses of a heavy neutral Higgs and vectorlike leptons up to 2 TeV and 1.5 TeV, respectively. Even for low $\tan\beta \gtrsim 1$, the analysis retains sensitivity to heavy Higgs masses slightly above 1 TeV. The future sensitivities at the HL-LHC extend the reach for heavy Higgses and new leptons to 2.7 TeV and 2 TeV, respectively.

Keywords: Multi-Higgs Models, Vector-Like Fermions

ArXiv ePrint: 2204.13272

https://doi.org/10.1007/JHEP10(2022)138

JHEP10(2022)138

Contents

JHEP10(2022)138

1 Introduction

Since the discovery of the Higgs boson, unveiling the Higgs sector involved in electroweak symmetry breaking (EWSB) has become a strong focus of the LHC program and is essential to understanding possible features of new physics beyond the Standard Model (SM). In particular, there are no symmetry arguments prohibiting the existence of an additional isodoublet field in the Higgs sector. Two Higgs doublet models (2HDMs) are generally considered to be among the simplest and theoretically well-motivated frameworks for possible extensions of the Higgs sector, for a review see, e.g. refs. [1, 2]. Popular examples of new theories beyond the SM (BSM) sharing this 2HDM-like Higgs sector include the Minimal Supersymmetric SM (MSSM) [3, 4], the DFSZ axion model [5, 6], and Twin Higgs model [7].

Another possibility which is not forbidden by any symmetry arguments is the existence of extra fermions beyond the three generations of the SM. Since the existence of new chiral fermions is strongly disfavored both by theoretical and experimental reasons [8], extra matter fermions, if they exist, are likely to be vectorlike with masses which can be generated independently of the Higgs mechanism. Vectorlike fermions have also been considered in many compelling BSM theories including both non-supersymmetric and supersymmetric

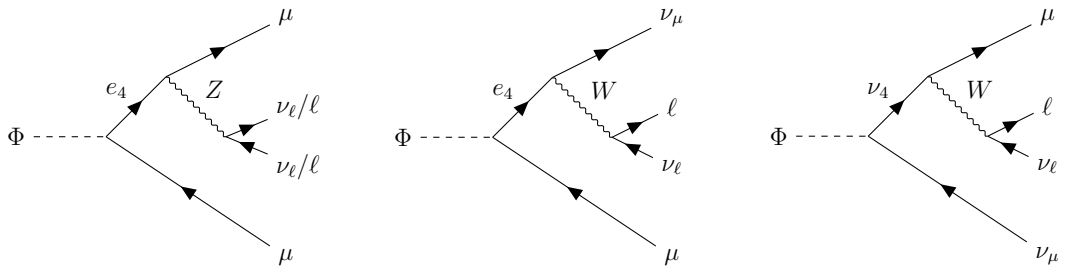

Figure 1. Leptonic cascade decays of a heavy neutral scalar (Φ) through a charged (e_4) and neutral (ν_4) vectorlike lepton. The decay in the left panel contributes to the $3/4\ell$ search if $Z \to \ell\ell$, while the other decay modes contribute to the $2\ell + E_T^{\rm miss}$ channel. The diagrams are drawn by TikZ-FeynHand [37, 38].

models with complete vectorlike families [9–13], composite/little Higgs model [14, 15], the KSVZ axion model [16, 17], and gauge mediated supersymmetry breaking model [6, 18–23]. Furthermore, models that include both an extension of the Higgs sector and vectorlike leptons were recently studied as possible solutions for the discrepancy in the measured value of the muon anomalous magnetic moment [24–27].

Existing searches at the LHC for extra Higgs bosons or vectorlike fermions have been developed independently. On the other hand, it has been proposed that signatures involving both types of new particles simultaneously have many advantages over the typical searches [28–36]. In particular, heavy Higgs cascade decays through a vectorlike lepton mixing with the SM fermion, such as those depicted in figure 1, provide relatively clean and distinctive signals due to their unique event topology. The final states of the processes in figure 1 are fully leptonic, possibly with missing energy, and hence we dub these signatures *leptonic cascade decays* throughout this paper. An important feature of our process is that the signature is "di-boson-like" but with one lepton pair whose momentum does *not* reconstruct the mass of a gauge boson in any way.

In this paper, we obtain new, model-independent constraints on heavy scalars and vectorlike leptons by recasting recent results of the dilepton with missing energy ($2\ell + E_T^{\rm miss}$) search [39] and 3 or 4 lepton ($3/4\ell$) search [40] at the LHC run2. We show that, remarkably, even with current data assuming a 50% cascade branching ratio the sensitivity to masses of new scalars and heavy leptons can reach well above 1 TeV, proving the effectiveness of our leptonic cascade processes. Our analysis results are quite promising compared to the typical consensus that the sensitivities for new leptons are weaker than those for vectorlike quarks considering the conventional production processes through gauge bosons.[1] For concreteness, we interpret our results in the context of a reference model: a two Higgs doublet model (2HDM) type-II, where $\Phi = H$ (A) is the heavy CP even (odd) neutral Higgs boson, augmented by vectorlike leptons which mix with the muon with e_4 (ν_4) being the lightest charged (neutral) vectorlike lepton. This is exactly the scenario which can explain the muon anomalous magnetic moment, even with multi-TeV Higgs bosons and new leptons [26, 27]. This is the main motivation to pursue signals with muons in the final state.

[1]For example, compare ref. [41] and [42].

JHEP10(2022)138

However, results generated from vectorlike leptons mixing with the first generation would be almost identical. We find that the projected sensitivity of the analysis for the HL-LHC extends the reach for heavy Higgses and new leptons to 2.7 TeV and 2 TeV, respectively. We emphasize that the search strategies and results in this paper can be readily applied to other new physics scenarios with the same kinematic topology and final states such as models of vectorlike leptons with a Z' boson [43–46], singlet-extended 2HDM or Next-to-MSSM type models [47].

This paper is organized as follows. In section 2, we outline search strategies at the LHC for the leptonic cascade decays. In section 3, we obtain model-independent current and projected upper limits on the proposed cross sections. The limits on the reference model, 2HDM with vectorlike leptons, are obtained in section 4. The results of our simulation at the benchmark points are tabulated in appendix A. Section 5 is devoted to our conclusions and outlooks. Details of the 2HDM we consider are explained in appendix B.

2 Search strategies

In this section, we provide a detailed description of the analysis strategies we propose to obtain new constraints for heavy scalars and new leptons based on the full LHC run2 data and projected expectations for the HL-LHC. We recast existing searches for leptonic signals in $2\ell + E_T^{\rm miss}$ and $3/4\ell$ final states initially motivated in supersymmetric and seesaw models. In this paper, we consider a simplified set-up with a scalar field and extra leptons, which allows the cascade decays shown in figure 1. The relevant Yukawa and gauge interactions in terms of the mass eigentstates (e_4, ν_4) include

$$\begin{aligned}\mathcal{L} \supset & -\Phi\left(y^{\Phi}_{4\mu}\overline{e}_{4R}\mu_L + y^{\Phi}_{4\nu}\overline{\nu}_{4R}\nu_L\right) + Z_\mu\left(\overline{e}_{4L}\gamma^\mu g^{Z_L}_{4\mu}\mu_L + \overline{e}_{4R}\gamma^\mu g^{Z_R}_{4\mu}\mu_R\right) \\ & + W_\mu\left(\overline{\nu}_{4L}\gamma^\mu g^{W_L}_{4\mu}\mu_L + \overline{\nu}_{4R}\gamma^\mu g^{W_R}_{4\mu}\mu_R\right) + h.c.\,,\end{aligned} \tag{2.1}$$

where Φ is the heavy scalar particle. We assume that the scalar field Φ is produced by the dimension-5 operator with gluons $(\phi/\Lambda)G^a_{\mu\nu}G^{a\mu\nu}$ or the Yukawa coupling with bottom quarks $y_b\phi\bar{b}b$ motivated by the 2HDM [2], where $G^a_{\mu\nu}$ is the field strength of gluons with an $\mathrm{SU}(3)_C$ index $a = 1, 2, \cdots, 8$. Here, Λ and y_b are the cut-off scale of the dimension-5 operator and Yukawa coupling constant, respectively.[2] For simplicity, events for SM background processes are taken from data available from existing results, giving the relevant references along the way. Nevertheless, as we will see our approach provides powerful enough experimental sensitivities on our leptonic cascade processes, as will be shown in section 4. Although not implemented here, further investigation for multiple lepton resonances in the $3/4\ell$ channel would increase the sensitivities even more, as already demonstrated in another cascade process in ref. [31].

[2]The dimension-5 operator is induced by quark loops, and the cut-off scale is given by [48]

$$\frac{1}{\Lambda} = \frac{\alpha_s y^{\phi}_Q}{12\sqrt{2}\pi m_Q},$$

for $m_Q \gg m_\phi$, where m_Q being a mass of a heavy quark Q and y^{ϕ}_Q is a Yukawa coupling constant for $\phi\overline{Q}Q$.

JHEP10(2022)138

2.1 $2\ell + E_T^{\rm miss}$ channel

All three leptonic cascade processes in figure 1 contribute to the $2\ell + E_T^{\rm miss}$ channel. We recast bounds for slepton and chargino masses in SUSY models from ref. [39] whose signal region includes a lepton pair which does not reconstruct the mass of a weak gauge boson.

Let us first explain how we obtain the sensitivities. We calculate the 95% $\mathrm{CL_s}$ limits by requiring [49]

$$\mathrm{CL}_s(\mu = 1) := \frac{\mathrm{CL}_{s+b}}{\mathrm{CL}_b} = \frac{1 - F\left(\sqrt{q_\mu^{\rm obs}}\right)}{F\left(\sqrt{q_\mu^A} - \sqrt{q_\mu^{\rm obs}}\right)} < 0.05, \tag{2.2}$$

where F is the cummulative distribution function of the normal distribution.

Here, the asymptotic formula for the distribution of test statistic q_μ, defined as

$$q_\mu = -2\log\frac{L\left(\mu, \hat{\hat{b}}\right)}{L\left(\hat{\mu}, \hat{b}\right)}, \tag{2.3}$$

is used [50], where the likelihood function is defined as:

$$L\left(\mu, b\right) = \prod_i \frac{\nu_i^{n_i}}{n_i!} e^{-\nu_i} \times \frac{1}{\sqrt{2\pi\sigma_i^2}} \exp\left[-\frac{(b_i - b_i^0)^2}{2\sigma_i^2}\right]. \tag{2.4}$$

In the above definition, $\nu_i = \mu s_i + b_i$ with s_i, b_i^0, σ_i being the number of signal events, the number of background events and the error of background in the i-th bin, respectively. Here, we assume that only background events have uncertainties and obey the Gaussian distribution.[3] $(\hat{\mu}, \hat{b})$ are the values of μ and $\hat{b} = \{\hat{b}_i\}$ which maximize the likelihood, and $\hat{\hat{b}} = \{\hat{\hat{b}}_i\}$ is the value of b_i for a given μ. Note that n_i corresponds to the observed data (central values of backgrounds) for $q_\mu^{\rm obs}$ (q_μ^A). For future limits, the significance for exclusion is given by [50]

$$Z_{\rm excl} \simeq \sqrt{q_{\mu=1}^{n=b}}\,, \qquad n_i = b_i\,, \tag{2.5}$$

while that for discovery is given by

$$Z_{\rm disc} \simeq \sqrt{q_{\mu=0}^{n=s+b}}\,, \qquad n_i = s_i + b_i\,. \tag{2.6}$$

For the future sensitivity with 3 ab^{-1} data, the number of events (error) are rescaled by $R_{\mathcal{L}}$ ($\sqrt{R_{\mathcal{L}}}$).

In ref. [39], the number of observed events, fitted SM backgrounds, and their uncertainties are listed in 4 categories of signal regions (SRs): `SR-SF-0J`, `SR-SF-1J`, `SR-DF-0J`, and

[3] In the $2\ell + E_T^{\rm miss}$ search [39], for supersymmetric particles, the uncertainties from the signal acceptance and shape are negligible, and the source for the signal uncertainty is from the signal cross sections. These are about 6% and are sub-dominant against the background uncertainties. In the $3/4\ell$ search [40], the uncertainties from the signals in the type-III seesaw and doublly charged Higgs bosons are not larger than a few percent. Thus, we assume that the uncertainties in our model are also sub-dominant compared with those from backgrounds.

JHEP10(2022)138

Signal Region	SR-SF-0J	SR-SF-1J	SR-DF-0J	SR-DF-1J
$n_{\text{non-b-tagged jets}}$	$= 0$	$= 1$	$= 0$	$= 1$
$m_{\ell_1\ell_2}$ [GeV]	> 100		> 121.2	
E_T^{miss} [GeV]	> 110			
$n_{\text{b-tagged jets}}$	$= 0$			

Table 1. Definitions of the signal regions (SRs) in the $2\ell+E_T^{\text{miss}}$ search. We do not consider the cut by E_T^{miss} significance which would have minor impacts on the signals. Each SR are binned by m_{T2} [GeV] as, $[100, 105]$, $[105, 110]$, $[110, 120]$, $[120, 140]$, $[140, 160]$, $[160, 180]$, $[180, 220]$, $[220, 260]$, $[260, \infty)$.

SR-DF-1J, further binned by m_{T2}.[4] The definitions of the SRs are summarized in table 1. The results in the last bin $m_{T2} > 260$ GeV are the most relevant ones constraining our parameter choices of heavy new particles.[5] Here, SF (DF) means that the two leptons in the final state are the same (different) flavor.

The number of signal events in each m_{T2} bin is calculated as

$$s_i = \mathcal{L} \times \sum_{\Phi} \sum_{P=\text{gg,bb}} \sum_{J=\text{EZ,EW,NW}} \sigma_{P\Phi} \times \text{Br}_{\Phi,J} \times \epsilon_i^{J,P}, \tag{2.7}$$

where $\mathcal{L}$ is the integrated luminosity. Here, Φ, P and J run over scalar fields, production process and decay modes, respectively. The cut acceptance times the detector efficiency, $\epsilon_i^{J,P}$, is a function of the scalar and new fermion masses and is the fraction of events that pass the cuts in a given signal region. From now on, we simply call the $\epsilon_i^{J,P}$ values the efficiencies. These are calculated by means of Monte Carlo simulations. In our analysis, we generated events using MadGraph5_2_8_2 [52] based on a UFO [53] model file generated with FeynRules_2_3_43 [54, 55]. In order to boost up the speed of the simulation, decays of the neutral heavy Higgs boson are handled using MadSpin [56]. Showering and hadronization are controlled by PYTHIA8 [57], and detector simulation by Delphes3.4.2 [58]. We used the default ATLAS card for the fast detector simulation.[6] Jets are reconstructed using the anti-k_T algorithm [59, 60] with $\Delta R = 0.4$. For the decay modes J = EZ, EW and NW, which are depicted from the left-to-right panels respectively in figure 1, we simulate the processes

$$pp \to \Phi + \text{jets}, \qquad \Phi \to \mu e_4 \, (\to \mu Z_\ell)\,, \tag{2.8}$$

$$pp \to \Phi + \text{jets}, \qquad \Phi \to \mu e_4 \, (\to \nu_\mu W_\ell)\,, \tag{2.9}$$

$$pp \to \Phi + \text{jets}, \qquad \Phi \to \nu_\mu \nu_4 \, (\to \mu W_\ell)\,, \tag{2.10}$$

where V_ℓ ($V = Z, W$) indicates leptonic decays including τ leptons.[7] Production of Φ is simulated via the CP-even Higgs boson production from gluon-gluon fusion in the 4 flavor

[4] We use the values of m_{T2} defined in ref. [51].

[5] In the bin with $m_{T2} > 260$ GeV, the fitted backgrounds are 6.8 ± 2.7, 8.0 ± 2.7, 2.9 ± 0.5 and 2.7 ± 0.8 for SR-SF-0J, SR-SF-1J, SR-DF-0J, and SR-DF-1J, respectively [39]. Hence the uncertainties are about 15% (30%) for the 0-jet (1-jet) SRs.

[6] In the ATLAS card, the reconstruction efficiency for electrons and muons with $p_T > 10$ GeV is 0.95 (0.85) for $|\eta| \leq 1.5$ ($1.5 < |\eta| \leq 2.5$), where η is the pseudorapidity. For the isolation, $R = 0.5$, $p_T^{\text{min}} = 0.5$ GeV and $I_{\text{min}} = 0.12$ (0.25) for electron (muon), see ref. [58] for the definitions of the variables R, p_T^{min} and I_{min}.

[7] Note that we include the contributions of the leptonic taus to the final states of our interest.

JHEP10(2022)138

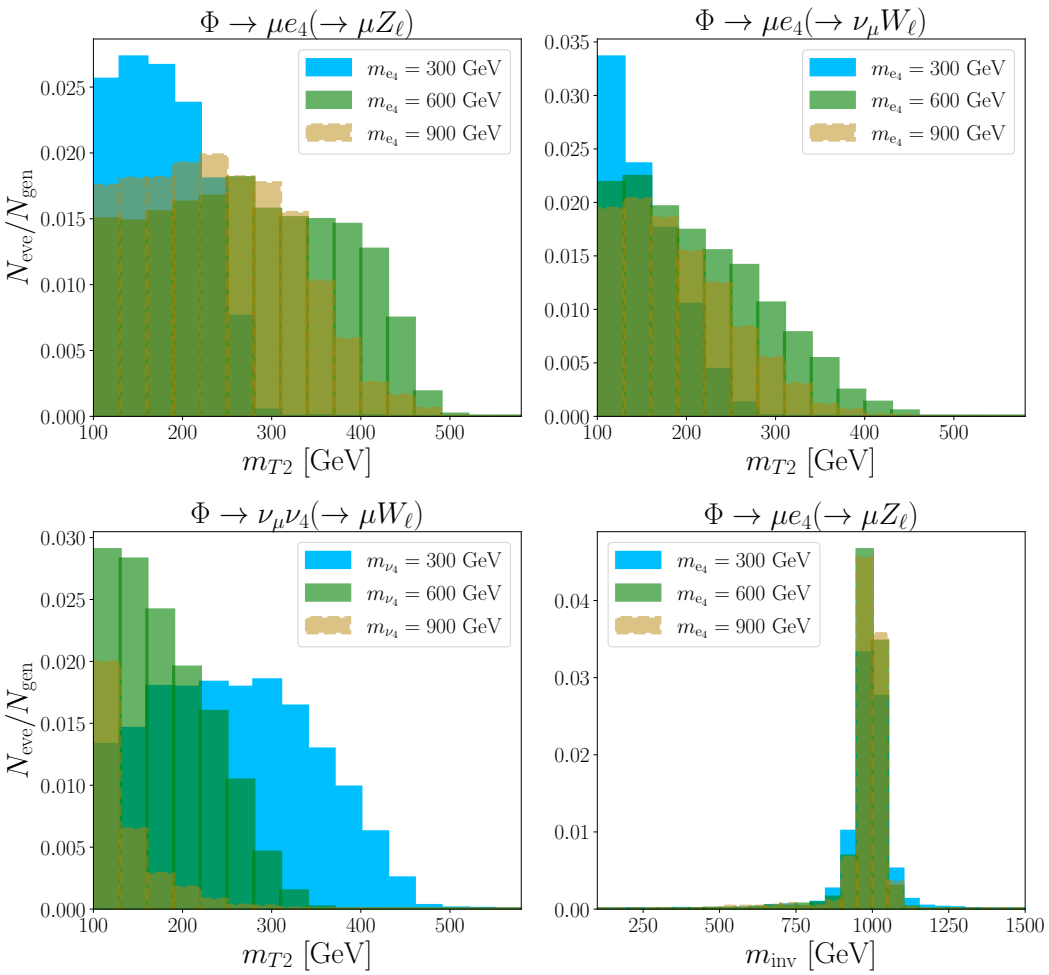

Figure 2. m_{T2} distributions of the Higgs cascade decays for $m_H = 1000$ GeV and vectorlike lepton masses 300, 600, and 900 GeV. The left-lower panel shows the invariant mass of four leptons from the EZ decay.

scheme with the 5-dimensional effective interaction and the b-annihilation process in the 5 flavor scheme separately. In the simulation up to two additional partons are included and these are matched to the showered events by the MLM matching [61] with `xqcut` $= m_H/10$.

The m_{T2} distributions from our leptonic cascade decays are shown in figure 2. We see that m_{T2} has a relatively sharp edge for lighter e_4 masses in the EZ and EW decays where all the $E_T^{\rm miss}$ comes wholly from the decay products of e_4, while the behavior is the other way around in the NW decay. Thus, the m_{T2} cuts can also be efficient in a wide range of parameter space in discriminating the leptonic cascade decays from the SM backgrounds, in particular for WW and $t\bar{t}$ events whose m_{T2} distributions are mostly shifted below ~ 160 GeV in all the SRs (See figure 5 of ref. [39].).

Among the m_{T2} bins, the highest bins with $m_{T2} > 260$ GeV are the most important to discriminate the signals from SM backgrounds. From the $gg\Phi$ ($bb\Phi$) production followed by the EZ decay, the efficiencies to the $m_{T2} > 260$ GeV bins are roughly 1-5% (5-10%) in

JHEP10(2022)138

Region	n_ℓ	$E_T^{\rm miss}$ [GeV]	Z-pairs	Other
3ℓ	$= 3$	< 50	1	veto if $m_T < 80$ GeV for off-Z ℓ
	$= 3$	> 50	1	veto if $m_T < 80$ GeV for off-Z ℓ
	$= 3$	< 50	0	veto if $m_T < 40$ GeV for off-flavor ℓ
	$= 3$	> 50	0	veto if $m_T < 40$ GeV for off-flavor ℓ
4ℓ	$= 4$	< 50	1	-
	$= 4$	> 50	1	-
	$= 4$	-	0	-

Table 2. Definitions of the signal regions in the $3/4\ell$ search [40]. The 3ℓ (4ℓ) SRs are further divided by into $m_{\rm inv}$ [GeV] $\in [0, 200]$, $[200, 400]$, $[400, 600]$, $[600, \infty)$ ($[0, 400]$, $[400, \infty)$). The off-Z ℓ is a lepton not in the Z-pair, and the off-flavor ℓ is a lepton whose flavor is different from the other two leptons. The cut for off-flavor ℓ is not applied if three leptons have the same flavor.

SF-0J, and 5-10% (5-10%) in SF-1J, where nJ ($n = 0, 1$) is the number of jets in the SRs. The efficiencies obtained in our simulation at a benchmark point are shown in appendix A.

2.2 $3/4\ell$ channel

Leptonic cascade decays involving the Z boson, i.e., the left-most panel of figure 1 (the EZ mode), can produce fully leptonic final states when including $Z \to \ell\ell$, which yields clear multiple leptonic resonance signals. The process is hence constrained by the searches for $3/4\ell$ events depending on the cuts for the softest lepton. For this analysis, we recast the search results of ref. [40]. The definitions of the SRs are summarized in table 2.

Among the SRs defined in ref. [40], the 4ℓ SRs with one Z-pair and small $E_T^{\rm miss}$ have the strongest sensitivities,[8] although there could be sub-dominant contributions from the other SRs due to the mis-reconstruction of leptons. There are two bins with $m_{\rm inv} < 400$ GeV and $m_{\rm inv} > 400$ GeV, where $m_{\rm inv}$ is an invariant mass of the four leptons, which corresponds to the mass of the neutral Higgs Φ in our reference model. This is shown in the lower-right panel of figure 2, where the events are clearly clustered around $m_\Phi = 1$ TeV. Since all SRs in ref. [40] are mutually exclusive, we combine them all in the same way as in the $2\ell + E_T^{\rm miss}$ search. The efficiencies of the EZ decay in the SR requiring four leptons, with one Z-like lepton pair with $E_T^{\rm miss} < 50$ GeV and $m_{\rm inv} > 400$ GeV are roughly 5-10% for both $gg\Phi$ and $bb\Phi$ productions. The efficiencies obtained in our simulation at a benchmark point are shown in appendix A.

3 Model independent limits on cross sections

We present the current limits based on the LHC run2 data with 139 fb^{-1} integrated luminosity and future prospects at the HL-LHC with luminosity 3 ab^{-1} based on the analysis strategies explained in the previous section. We emphasize that our analysis results

[8] In these signal regions, the fitted backgrounds are 169 ± 8 (36.5 ± 2.1) for $m_{\rm inv} < 400$ GeV (> 400 GeV).

JHEP10(2022)138

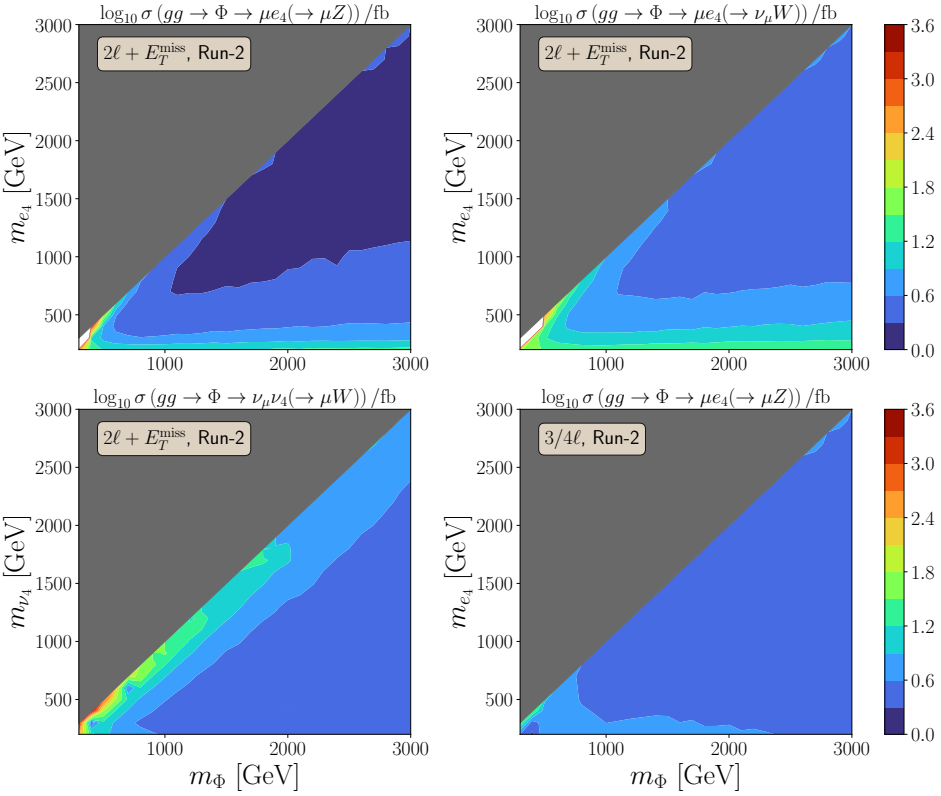

Figure 3. Current upper bounds on $\sigma(gg \to \Phi \to \ell\ell_4(\to \ell' V))$ from our recast of the $2\ell + E_T^{\rm miss}$ and $3/4\ell$ searches. See the texts for the details.

can be generically applied to other BSM scenarios which share the same kinematic topology and final states; thereby model-independent upper limits and prospects on the total cross sections will be shown first. For scenarios with a resonant particle production like a Higgs boson, i.e., via gluon-gluon fusion and/or b-annihilation, our results on the branching ratios can be readily applied. Finally, we provide the model-dependent constraints and expected sensitivities for the vectorlike lepton mass and heavy neutral Higgs mass in a 2HDM type-II.

Figures 3 (5) and 4 (6) show the current (future) upper limits on

$$\sigma\left(gg \to \Phi + \text{jets}\right) \times \text{Br}\left(\Phi \to \ell\ell_4\left(\to V\ell'\right)\right) , \tag{3.1}$$

and

$$\sigma\left(b\bar{b} \to \Phi + \text{jets}\right) \times \text{Br}\left(\Phi \to \ell\ell_4\left(\to V\ell'\right)\right) , \tag{3.2}$$

respectively.[9] Here, $(\ell_4, \ell, V, \ell') = (e_4, \mu, Z, \mu)$, (e_4, μ, W, ν_μ), (ν_4, ν_μ, W, μ) refers to the EZ, EW and NW decays, respectively. Tables of the values used in these figures are attached in supplemental material. Note that the production and decays of Φ are handled separately by `MadGraph` and `MadSpin` respectively to boost up the speed of our event generations; thereby

[9] In the small white region at $m_H \sim m_{e_4} \lesssim 400$ GeV, the efficiencies in all of the signal regions of the $2\ell + E_T^{\rm miss}$ search are zero according to our simulation.

JHEP10(2022)138

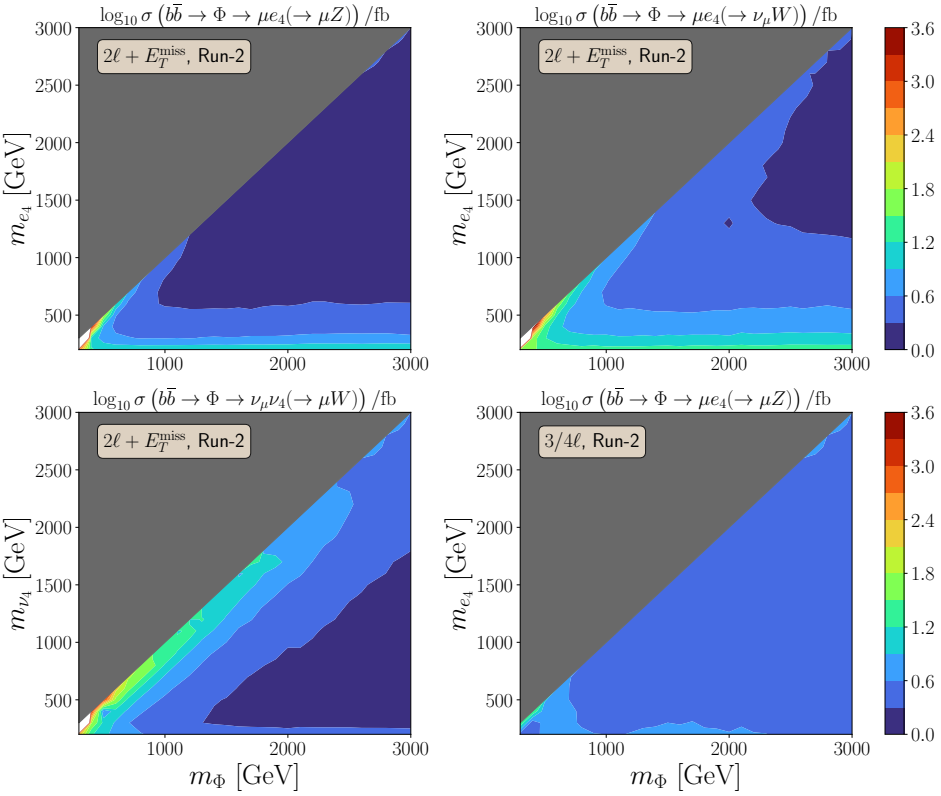

Figure 4. Current upper bounds on $\sigma(b\bar{b}\to\Phi\to\ell\ell_4(\to\ell' V))$.

our method does not technically include the cases of an off-shell production of Φ or the breakdown of the narrow width approximation, which might provide different values of the cut acceptances. The number of signal events in the i-th m_{T2} bin is calculated by

$$s_i = \mathcal{L}\times\sigma_{P\Phi}\times \mathrm{Br}_{\Phi,J}\times\epsilon_i^{J,P}\,, \tag{3.3}$$

without summations for each choice of Φ, J, P, and we obtain upper limits on $\sigma_{P\Phi}\times\mathrm{Br}_{\Phi,J}$.

The current limits are $\mathcal{O}\,(1{-}10)$ fb for $m_\Phi \gtrsim 1$ TeV for the EZ and EW decay modes. The search is more sensitive for larger m_{e_4} due to the increasing number of events passing the m_{T2} cut for larger lepton masses, as displayed in figure 2. The limits on the NW mode is of the same order, but the search is more sensitive to the smaller m_{ν_4} since the m_{T2} distribution shows the opposite behavior with the vectorlike lepton mass. In both cases the sensitivities increase with increasing m_Φ as a larger scalar mass tends to produce events with larger values of m_{T2}. The bottom-right panels in figures 3–6 show limits on the EZ mode, where $Z\to\ell\ell$, which is constrained by the $3/4\ell$ search channel. The limit is almost independent with respect to the vectorlike lepton mass because $m_{\rm inv}$ is determined by m_Φ, so the only requirement is that four leptons should be reconstructed with a sufficient p_T. At the HL-LHC, we expect the experimental sensitivities to the cross sections would be increased by about $\sqrt{R_\mathcal{L}}\simeq 4.7$ and hence they can be improved to be $\mathcal{O}\,(0.2-1)$ fb.

JHEP10(2022)138

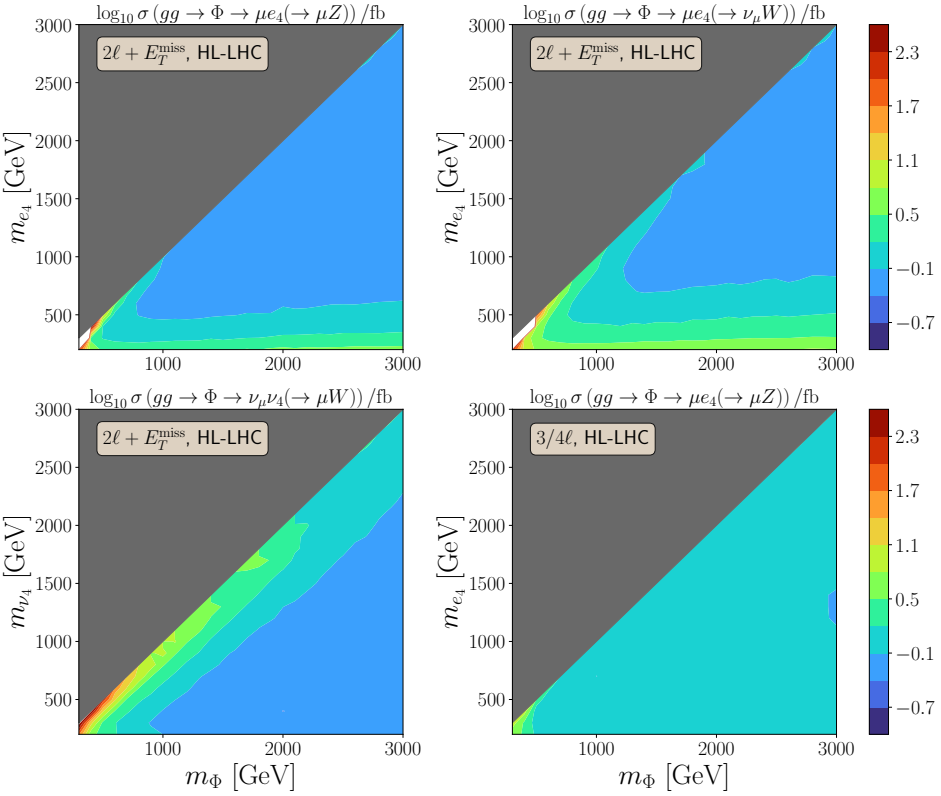

Figure 5. Projected upper bounds on $\sigma(gg \to \Phi \to \ell\ell_4(\to \ell' V))$ at the HL-LHC. See the texts for the details.

4 2HDM with vectorlike leptons

In this section, we apply our results to the reference model: a 2HDM type-II augmented by vectorlike leptons. The details of our reference model are described in refs. [28, 30] but we simply show the Lagrangian and explain the field contents briefly to aid with our discussion. The most general Lagrangian of Yukawa interactions and mass terms relevant for our processes include:

$$\begin{aligned}\mathcal{L} \supset & - y_\mu \bar{\mu}_L \mu_R H_d - \lambda_E \bar{\mu}_L E_R H_d - \lambda_L \bar{L}_L \mu_R H_d - \lambda \bar{L}_L E_R H_d - \bar{\lambda} H_d^\dagger \bar{E}_L L_R \\ & - \kappa_N \bar{\mu}_L N_R H_u - \kappa \bar{L}_L N_R H_u - \bar{\kappa} H_u^\dagger \bar{N}_L L_R \\ & - m_L \bar{L}_L L_R - m_E \bar{E}_L E_R - m_N \bar{N}_L N_R + \text{h.c.}\,, \end{aligned} \tag{4.1}$$

where the first term is the Yukawa interaction of the down-type Higgs boson H_d with the SM muon, followed by the Yukawa interactions with the vectorlike lepton isodoublet $L_{L,R} = (L^0_{L,R}, L^-_{L,R})$ and the charged isosinglet $E_{L,R}$ which have the same quantum numbers as SM leptons (denoted by various λ's). The second line denotes the Yukawa interactions between the up-type Higgs H_u and the neutral vectorlike leptons including a SM singlet lepton $N_{L,R}$ (denoted by κs). The final line denotes the vectorlike mass terms of the new leptons. In order to avoid strong bounds in the Higgs sector, we take the alignment limit [62–65], i.e., $\alpha = \beta - \pi/2$ where α is the neutral Higgs mixing angle and $\tan\beta = \langle H_u \rangle / \langle H_d \rangle$ is

JHEP10(2022)138

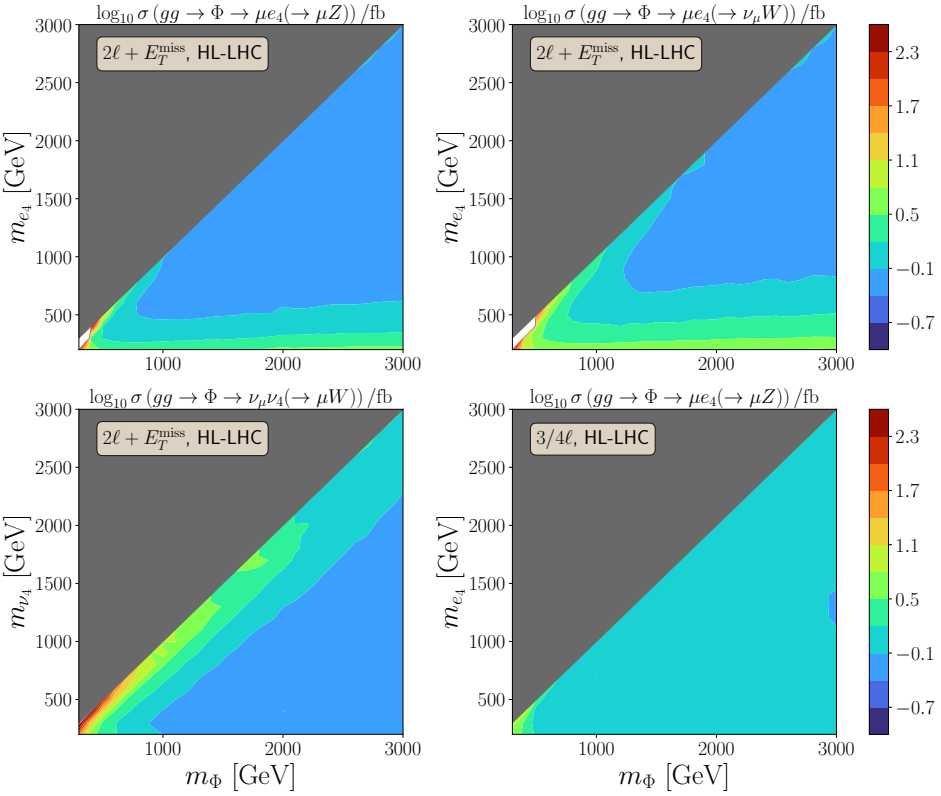

Figure 6. Projected upper bounds on $\sigma(b\bar{b} \to \Phi \to \ell\ell_4(\to \ell' V))$ at the HL-LHC.

the ratio of the vacuum expectation values of the two Higgs doublets. More details on the model, the field contents, mass mixing, and the interactions among the mass eigenstates are explained in ref. [28].

4.1 Heavy neutral Higgs to $\tau\tau$

Searches for heavy BSM Higgs bosons have been considered as important tasks in the LHC collaborations. Among the conventional searches for a heavy neutral Higgs boson decaying to the SM fermions, we impose constraints from the $\Phi \to \tau\tau$ searches [66, 67] which provides the most stringent limits in a wide range of parameter space (for example, see ref. [68]).

The neutral Higgs bosons dominantly decay to the SM fermions in the third generation. In our numerical analysis, we calculated $H \to cc$, bb, tt, $\tau\tau$, $\gamma\gamma$, gg, hh and $A \to cc$, bb, tt, $\tau\tau$, $\gamma\gamma$, gg, assuming the MSSM Higgs potential for $H \to hh$. Although not pursued in this paper, our results could be weakened upon further consideration of the Higgs potential where BR($H \to hh$) is sizable. The branching fractions involving weak gauge bosons are vanishing in the alignment limit and we do not consider those decay modes. Note, however, that our final states nevertheless mimic certain di-boson-like signals and hence can be potentially constrained using the corresponding searches proposed in [28–30].

We consider the limit on $\sigma \times \mathrm{Br}(\Phi \to \tau\tau)$ using the latest ATLAS data [67] for gluon-gluon fusion ($gg\Phi$) and b-annihilation ($bb\Phi$). In our analysis, the production of the neutral Higgs bosons, H and A, via these processes are calculated using `SuShi` [69, 70] and we further assume $m_H = m_A$ to avoid bounds from custodial symmetry breaking. Values of

JHEP10(2022)138

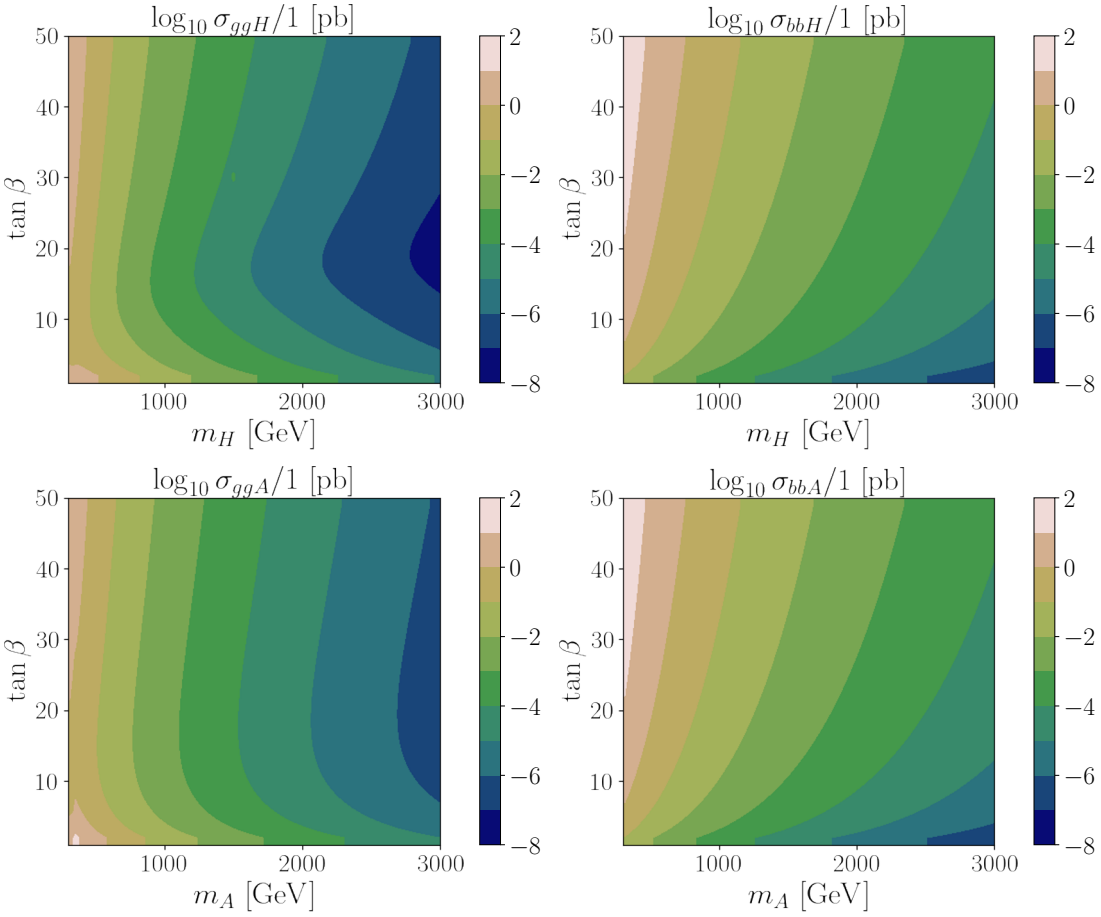

Figure 7. Production cross sections of the neutral Higgs bosons H (upper) and A (lower) via the ggF (left) and bbH (right) processes at $\sqrt{s} = 13$ TeV.

the production cross sections at $\sqrt{s} = 13\,\text{TeV}$ are shown in figure 7. For the constraints discussed later in our reference model, we use these values of production cross sections and consider a parameter set to be excluded if either

$$\sum_{\Phi=H,A} \sigma_{gg\Phi} \times \text{Br}\left(\Phi \to \tau\tau\right) \quad \text{or} \quad \sum_{\Phi=H,A} \sigma_{bb\Phi} \times \text{Br}\left(\Phi \to \tau\tau\right) \tag{4.2}$$

is larger than the experimental bounds on $\sigma \times \text{BR}\left(\Phi \to \tau\tau\right)$, where $\text{BR}\left(\Phi \to \tau\tau\right)$ is calculated in context of the model. In estimating the future sensitivity at the HL-LHC, we assume the statistical uncertainty dominates and simply rescale the upper bound on the cross section by $\sqrt{R_{\mathcal{L}}}$, where $R_{\mathcal{L}} := \mathcal{L}_{\text{run2}}/\mathcal{L}_{\text{HL}}$, to estimate the future sensitivity at the HL-LHC, where the integrated luminosities are $\mathcal{L}_{\text{run2}} = 139\ \text{fb}^{-1}$ and $\mathcal{L}_{\text{HL}} = 3\ \text{ab}^{-1}$.

4.2 Constraints on the branching fractions

We now discuss the constraints on the branching fractions of the neutral heavy Higgs bosons. Figures 8–11 show the upper bounds on the branching fractions from the current (future) data assuming a production cross section for Φ as in a 2HDM type-II for $\tan\beta = 10$ and

JHEP10(2022)138

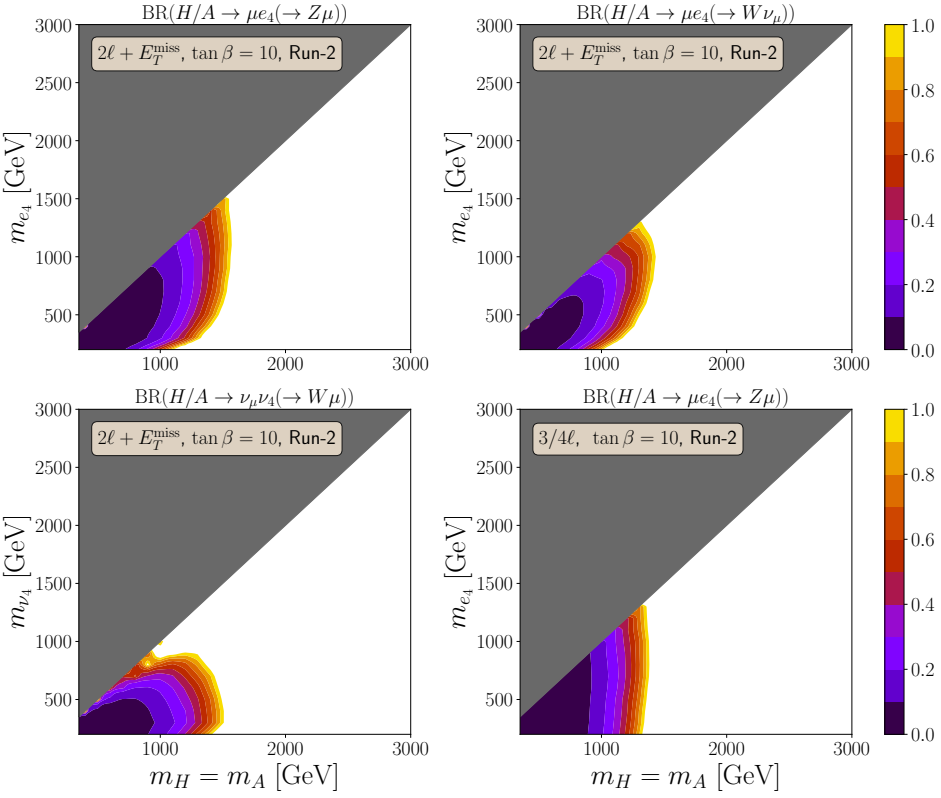

Figure 8. Current upper bounds on the branching fractions when $\tan\beta = 10$.

50, respectively. The number of signal events is calculated in a combined way by

$$s_i = \mathcal{L} \times \sum_{P,\Phi} \sigma_{P,\Phi} \times \mathrm{Br}_{\Phi,J} \times \epsilon_i^{J,P}, \tag{4.3}$$

where $\Phi = H, A$ and $P = gg, bb$, but there is no summation over the decay modes $J = \mathrm{EZ},\ \mathrm{EW},\ \mathrm{NW}$. The production cross sections from gluon fusion and b-annihilation are calculated using `SuShi` [69, 70]. In these figures, we neglect the difference in the branching fractions between the CP-even and CP-odd Higgs bosons, which is expected to be small for $m_t^2/m_H^2 \ll 1$, i.e., we set $\mathrm{Br}_H = \mathrm{Br}_A$. We assume that only one of the three decay modes contributes to the signal regions to extract the corresponding limit. Here, we also show the limits on the NW decay mode for completeness, although this branching fraction for a mostly singlet-like ν_4 is constrained to be below ~ 5 % (0.1 %) for $m_H \lesssim 340\,\mathrm{GeV}$ (above 340 GeV) in our reference model. This decay is constrained mainly by the $\Phi \to \tau\tau$ search results but also from electroweak precision measurements (see the discussion in appendix B.). The limits obtained by combining all decay modes are presented in the next subsection.

The $2\ell + E_T^{\rm miss}$ search excludes the Higgs boson mass up to about 1.3 (2.1) TeV for $m_{e_4} \gtrsim 500$ GeV and $\tan\beta = 10$ (50) if the branching fraction is 50%. The sensitivity of this search becomes weaker for smaller m_{e_4}, because the m_{T2} distribution drops off around m_{e_4} as shown in the top panels of figure 2, and hence cannot pass the m_{T2} cut. The limits for the EZ decay mode are tighter than those for the EW decay mode because of the broader m_{T2} distribution. For the NW decay, although the branching fraction cannot be sizable in our reference model, a similar range of Higgs masses can be probed unless the mass

JHEP10(2022)138

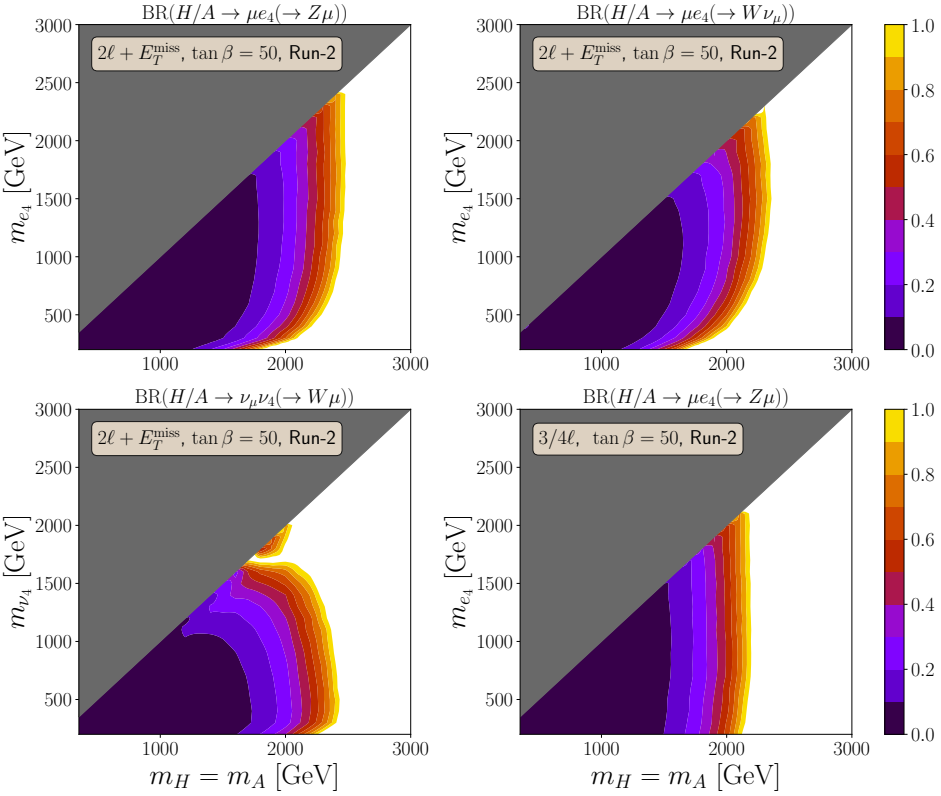

Figure 9. Current upper bounds on the branching fractions when $\tan\beta = 50$.

difference is small, implying a smaller m_{T2}. At the HL-LHC with 3 ab^{-1} data, the limits will be strengthened to about 1.8 (2.8) TeV for $\tan\beta = 10$ (50) and 50% branching fraction.

The limits on the branching fraction of the EZ decay mode from the $3/4\ell$ search are shown in the lower-right panels of figures 8–11. The current (future) sensitivities on m_H with the 50% total branching fraction are about 1.2 and 1.5 TeV (1.9 and 2.4 TeV) for $\tan\beta = 10$ and 50, respectively. These are nearly independent of the masses of the vectorlike leptons because the key kinematic cut is given by $m_{\rm inv} = m_\Phi$.

4.3 Limits on the model

Finally, we study constraints on the model in which the Lagrangian is given by eq. (4.1). In our numerical analysis, we scan the parameters to vary in the ranges:

$$m_H,\ m_L,\ m_E,\ m_N \in\ [300,\ 3000]\ \text{GeV}\,, \tag{4.4}$$

$$\lambda_L, \lambda_E, \lambda,\ \overline{\lambda},\ \kappa,\ \overline{\kappa} \in\ [-c_{\rm max}, c_{\rm max}]\,, \tag{4.5}$$

$$\tan\beta \in\ [1, 50]\,, \tag{4.6}$$

where we consider $c_{\rm max} = 1$ and $3.5 \sim \sqrt{4\pi}$, with the latter being motivated by the upper limit of couplings near the weak scale from perturbativity. Since there are many parameters in the Lagrangian above, we consider an optimized parameter scan strategy;

JHEP10(2022)138

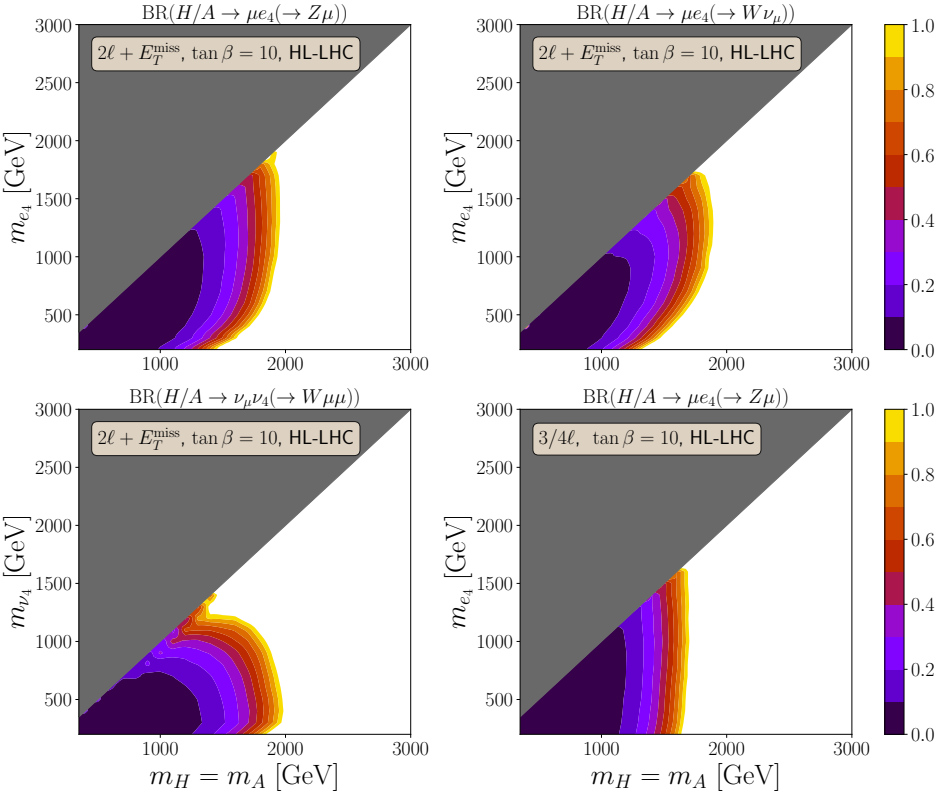

Figure 10. Future upper bounds on the branching fractions when $\tan\beta = 10$.

two representative cases maximizing BR($H \to e_4\mu$) are picked to focus on emphasizing the current and future sensitivities of our processes:

(1) light-L: $m_L < m_H < m_E, m_N$, $\kappa_N = 0$, $\lambda_L > 0.5$,

(2) light-E: $m_E < m_H < m_L, m_N$, $\kappa_N = 0$, $\lambda_E > 0.5$,

The "light-L" denotes the case where the lightest new leptons e_4, ν_4 are almost isodoublet, i.e., $(e_4^-, \nu_4) \sim (L^-, L^0)$. The "light-E" denotes the case where e_4 is almost isosinglet, i.e., $e_4 \sim E$. In order to focus on our leptonic cascade processes, we require the other vectorlike leptons to be heavier than the neutral Higgses, H/A. Note that these two representative cases correspond to the simple scenarios where the branching ratios of e_4 typically follow the pattern expected by the Goldstone boson equivalence theorem, i.e., BR($e_4 \to W\mu$):BR($e_4 \to Z\mu$):BR($e_4 \to h\mu$) = 2:1:1 (for isosinglet) and 0:1:1 (for isodoublet), and the approximation $(\lambda_L, \lambda_E, \lambda, \bar{\lambda})v/(m_L, m_E) \ll 1$ is valid in most of the parameter space; the couplings among the mass eigenstates are easily expressed with the Lagrangian parameters as in refs. [30, 71]. As pointed out in ref. [34] for the vectorlike quarks, general vectorlike lepton scenarios can include the possibilities of small λ_L/λ_E as well as sizable mixing between the isodoublet and isosinglet, which allow all the values between 0 and 1 for the e_4 branching ratios.

In the parameter scan, we do not study the case in which $\nu_4 \sim N$ when $\Phi \to \nu_4\nu_\mu \to W\mu\nu_\mu$ can dominate for $\kappa_N > 0.5$. This is because, in the limit where

JHEP10(2022)138

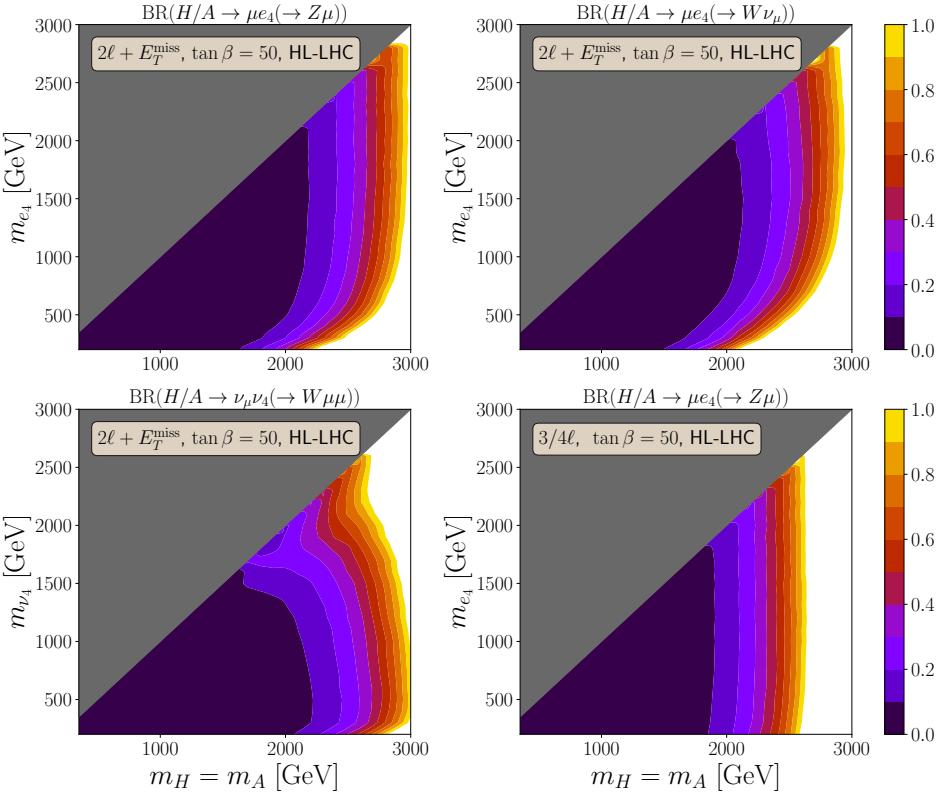

Figure 11. Future upper bounds on the branching fractions when $\tan\beta = 50$.

$(\lambda, \bar{\lambda}, \lambda_E, \lambda_L, \kappa, \bar{\kappa}, \kappa_N)v/(m_N, m_L) \ll 1$ is valid, large values of κ_N maximizing the decay width $\Phi \to \nu_4\nu_\mu$ are strongly constrained by the electroweak precision measurements, especially from the Fermi constant G_F at large $\tan\beta$.[10] Moreover, the values of BR($\Phi \to \nu_4\nu_\mu$) are limited by the competing decay modes, $\Phi \to \tau^+\tau^-$ and $\Phi \to t\bar{t}$, and hence we find the total values of BR($\Phi \to \nu_4\nu_\mu \to W\mu\nu_\mu$) are preferred to be smaller than 4%. See appendix B for more details.

In the light-L (light-E) case, we scan the absolute value of the Yukawa coupling constant λ_L (λ_E) in the $[0.5, c_{\rm max}]$ range, so that the branching fraction BR($\Phi \to e_4\mu$) covers the full range of possible values. For each point, we calculate the contributions to the electroweak precision observables (EWPOs), cross sections to the di-tau channels, CL$_s$, $Z_{\rm excl}$, and $Z_{\rm disc}$.

Note that the heavy Higgs Φ can decay into the vectorlike lepton pair, e.g., $\Phi \to e_4 e_4$, but the decay width is suppressed by $(\lambda_L, \lambda_E)v_u/(m_L, m_E)$ compared to that of $\Phi \to e_4\mu$ in our simple scenarios "light-L" and "light-E". Nevertheless, in general scenarios, such a double e_4 production can be sizable and provide another interesting signature, which is beyond the scope of this paper. Recall also that the vectorlike leptons can be pair produced through gauge boson interactions which can be subjected to robust bounds, as in ref. [41]. The most recent analysis by ATLAS in ref. [74] shows that a nominal bound of

[10] Although we use the constraints from the Particle Data Group [72], it is worth noting that the recent measurement of M_W from the CDF collaboration at Tevatron [73] claims a central value in tension with respect to other experiments as well as an increase in precision, which would give stronger bounds.

JHEP10(2022)138

$m_{e_4,\nu_4} \gtrsim 800\,\text{GeV}$ can be obtained assuming our total cross section of $pp \to e_4\nu_4 \to WW\nu_\mu\mu$ is similar to what is expected in the type-III seesaw model. We do not include this bound (after rescaling the production cross section) in our parameter scan but we emphasize that some light e_4 region can be constrained further by this complementary search.

The upper (lower) panels of figure 12 show the sensitivities of our reference model in the $2\ell + E_T^{\text{miss}}$ analysis for the light-E (light-L) case when $c_{\text{max}} = 1$. In the left panels, where the sensitivities are represented in the $m_H - m_{e_4}$ plane, the pink (2ℓ run2), green (2ℓ disc.) and blue (2ℓ excl.) points correspond to the regions which can be covered by our $2\ell + E_T^{\text{miss}}$ analysis with current data at 95% C.L., the corresponding discovery region at the HL-LHC, and the future exclusion region, respectively. Note that here exclusion regions mean that some choices of parameters would be excluded. We include the contributions from the three decay modes, EZ, EW and NW, as defined in eq. (2.7).

The points are plotted in the order given in the legend, i.e. pink points are plotted over green points, and green points over blue ones. In the right panels, we classify the blue points (2ℓ excl.) by whether they are expected to have sensitivity to the $\Phi \to \tau\tau$ search or not at the HL-LHC. The blue (2ℓ only) and cyan (2ℓ & $\tau\tau$) points are both within the future sensitivity of the $2\ell + E_T^{\text{miss}}$ channel but we expect the searches for $\Phi \to \tau\tau$ to also have sensitivity in the cyan region. The brown ($\tau\tau$ run2) points are excluded by the current $\tau\tau$ search, and the purple ($\tau\tau$ excl.) points correspond to the region we expect to be possibly excluded by the future $\tau\tau$ search at the HL-LHC but not by the future $2\ell + E_T^{\text{miss}}$ search. The white points (no excl.) are not excluded by any of the search channels discussed in this paper. The brown solid (purple dashed) line corresponds to the nominal exclusion limit from the current (future) sensitivity of $\Phi \to \tau\tau$ searches *without the presence of vectorlike leptons*. These nominal bounds can be pushed back to the brown or purple scattered dots in the presence of vectorlike leptons depending on the parameter choices. The (small) purple region in the top-right corner denotes the region within the reach of the $\tau\tau$ search but not of our leptonic cascade process.

We find the current search for the $2\ell + E_T^{\text{miss}}$ channel is sensitive to $m_\Phi \leq 1.7\,\text{TeV}$ and $m_{e_4} \leq 1\,\text{TeV}$ when $c_{\text{max}} = 1$ and the sensitivity to Higgs masses close to 1 TeV remains for any $\tan\beta > 1$. This is quite promising even compared to the conventional heavy Higgs search $\Phi \to \tau\tau$. Moreover the future sensitivities with 3 ab^{-1} extend to $m_\Phi \lesssim 2.2\,\text{TeV}$ and $m_{e_4} \lesssim 1.5\,\text{TeV}$ covering a much wider range of $\tan\beta$ than the conventional searches.

Figure 13 shows the corresponding sensitivities for the $3/4\ell$ search. The labels 4ℓ indicate that these are limits or sensitivities from the $3/4\ell$ search instead of the $2\ell + E_T^{\text{miss}}$ search. In the light-E case, the limit is much weaker than that from the $2\ell + E_T^{\text{miss}}$ search because the EW decay mode does not contribute to the SRs of the $3/4\ell$ search. While in the light-L case, the limit is similar because $\text{BR}\,(e_4 \to Z\mu)$ is larger than in the light-E case. We may be able to test whether the lightest charged vectorlike lepton e_4 is almost singlet-like or doublet-like by using both of $2\ell + E_T^{\text{miss}}$ and $3/4\ell$ channels in a complementary way. For example, if we were able to discover the signal at $m_\Phi = 1.7\,\text{TeV}$ and $m_{e_4} = 1\,\text{TeV}$ for $c_{\text{max}} = 1$ in both channels, the discovered e_4 should be almost doublet-like.

In order to demonstrate the maximal capability of our analysis, we also allow larger Yukawa coupling constants up to $c_{\text{max}} = 3.5$. The corresponding results are shown in figures 14 and 15. The branching fractions can be larger than those in the $c_{\text{max}} = 1.0$ case,

JHEP10(2022)138

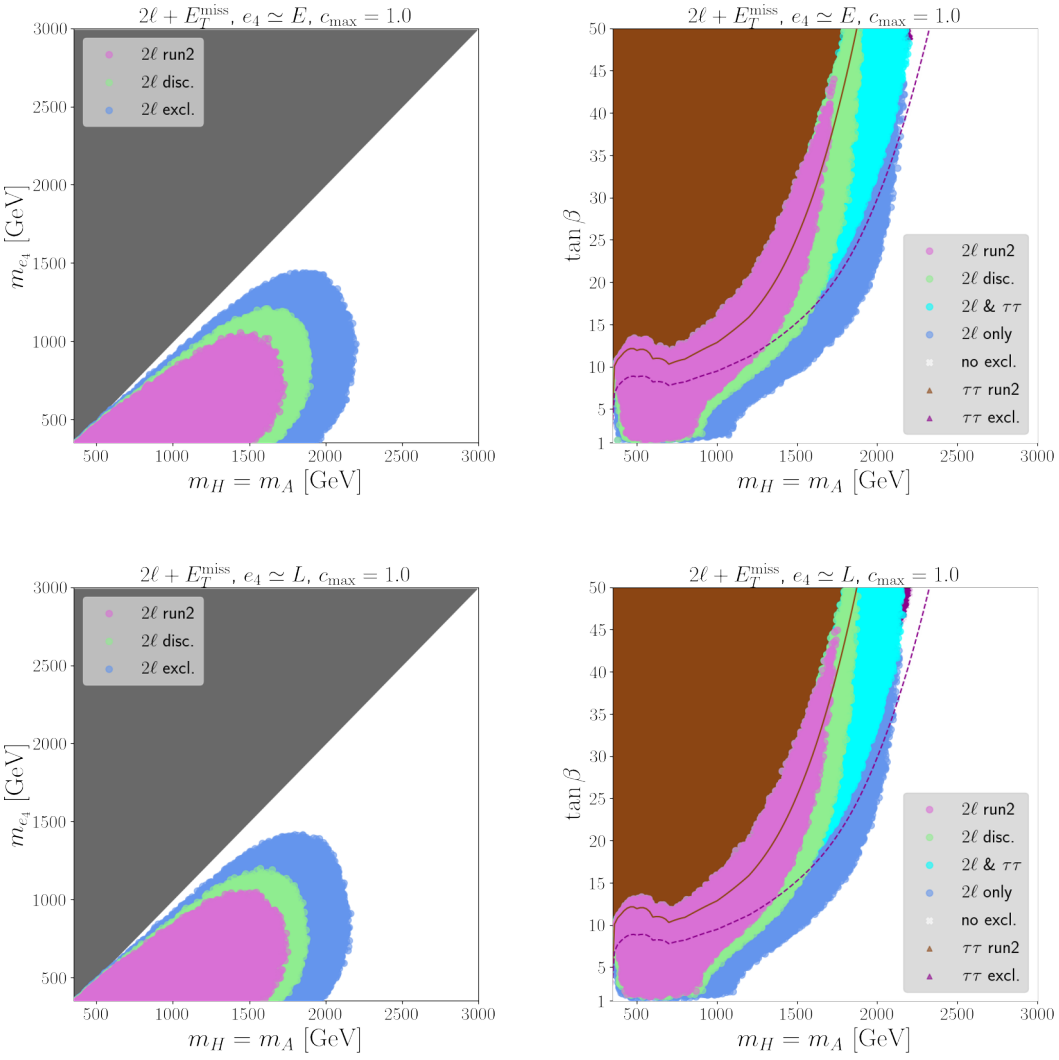

Figure 12. Sensitivities of the $2\ell + E_T^{\rm miss}$ search to the light-E (light-L) scenario with $c_{\rm max} = 1$ in the upper (lower) panels. In the labels, "2ℓ" is a short for $2\ell + E_T^{\rm miss}$ search and "$\tau\tau$" is the di-tau search. In addition, "run2", "disc." and "excl." indicate that the points are constrained by the current run-2 data, expected to be discovered and constrained by the future HL-LHC data, respectively. See the texts for more details.

and thus the searches can probe heavier mass regions: $m_\Phi \lesssim 2\,\text{TeV}$ and $m_{e_4} \lesssim 1.5\,\text{TeV}$ with current data, and $m_\Phi \lesssim 2.5\,\text{TeV}$ and $m_{e_4} \lesssim 1.8\,\text{TeV}$ at the HL-LHC. Note that the presence of vectorlike leptons with large couplings can significantly dilute the typical search for $H \to \tau\tau$ as seen by the absence of cyan points and purple triangles in figure 14 (where they are completely covered by the pink and green points) as compared to figure 12. We found that the $\tau\tau$ search at the HL-LHC can lose its sensitivity up to about the run2 limit, i.e. the brown solid line, due to the large Yukawa coupling constant λ_L or $\lambda_E \sim 3.5$. In that case, the leptonic cascade search strategy presented here is necessary to probe the details of the Higgs sector.

JHEP10(2022)138

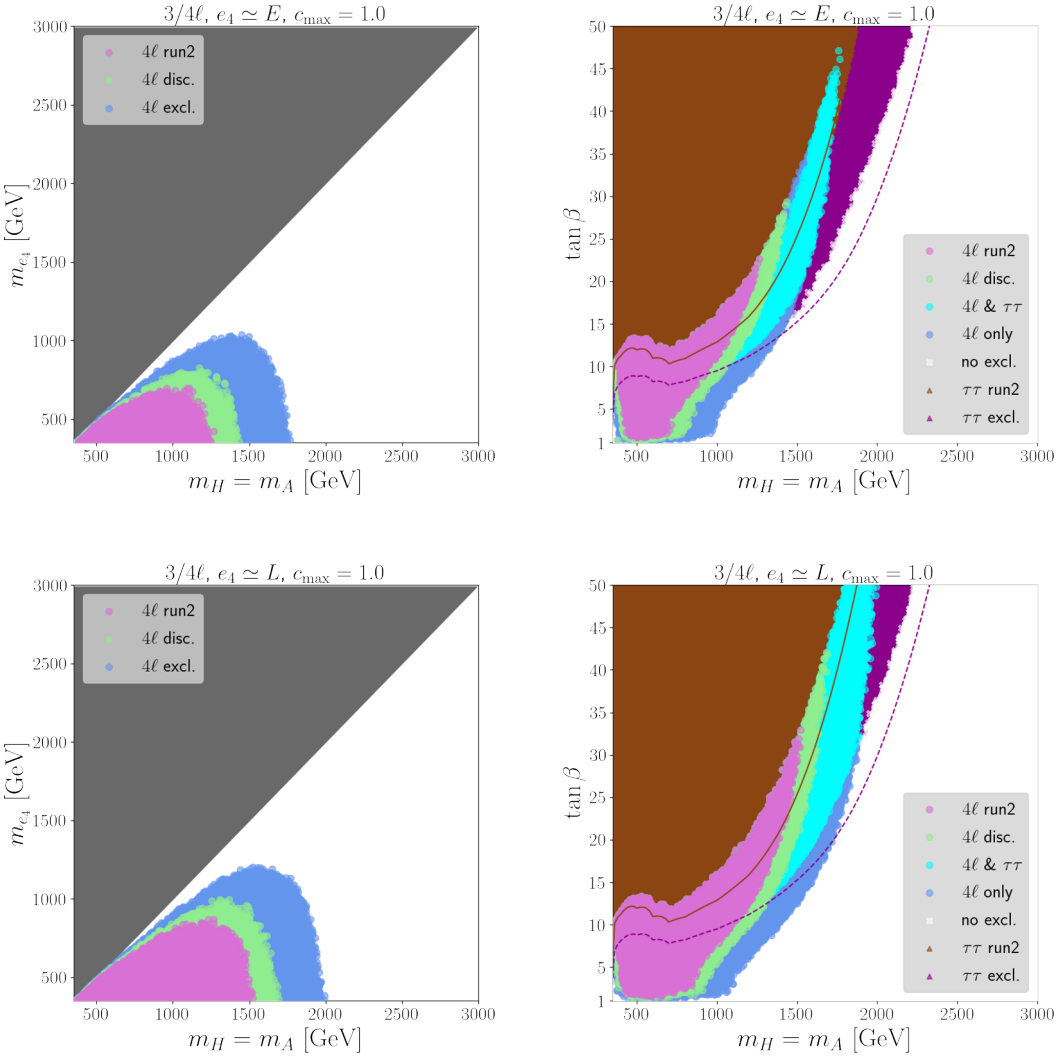

Figure 13. Sensitivities of the $3/4\ell$ search to the light-E (light-L) scenario with $c_{\max} = 1$ in the upper (lower) panels. In the labels, "4ℓ" is a short for $3/4\ell$ search and the rest of the labels are the same as those in figure 12.

5 Conclusion

In this paper, we have studied the potential of leptonic cascade decays of a heavy neutral Higgs boson through vectorlike leptons as a simultaneous probe of an extended Higgs sector and extra matter particles at the LHC. The fully leptonic final states contribute to multi-lepton signals such as $2\ell + E_T^{\text{miss}}$ and $3/4\ell$ which are already under investigation motivated by BSM scenarios such as SUSY and seesaw models. We have found that by simply recasting the existing searches we can obtain new strong constraints to any BSM scenarios sharing the same event topology and final states as our reference scenario, depicted in figure 1. Therefore, some of our analysis results are shown in *model independent* ways. The 95% C.L. model independent upper limits on the total cross sections are found to be

JHEP10(2022)138

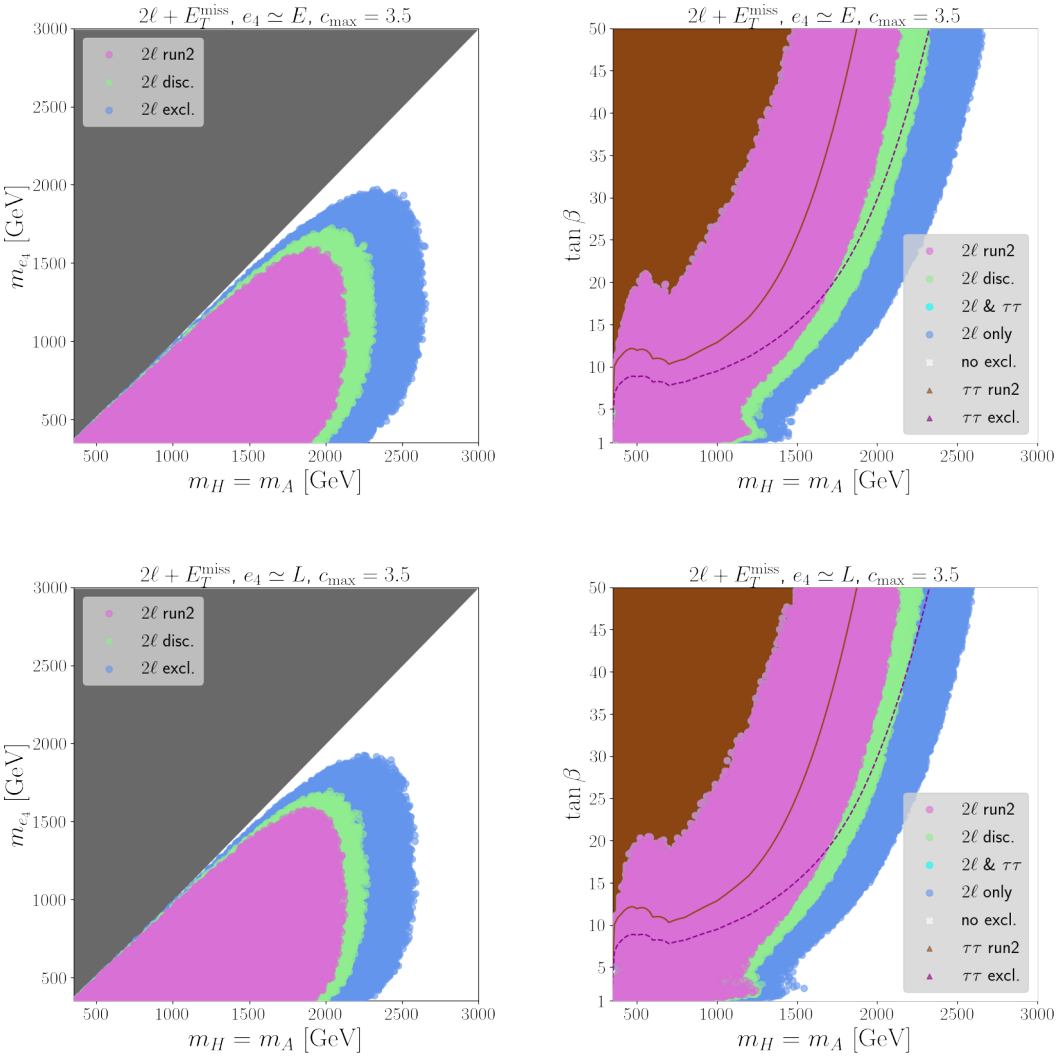

Figure 14. Sensitivities of the $2\ell + E_T^{\text{miss}}$ search to the light-E (light-L) scenario with $c_{\max} = 3.5$ in the upper (lower) panels. The labels are the same as those in figure 12.

$\mathcal{O}(1 - 10$ fb) for a heavy neutral Higgs (or a resonant particle producing the same topology) in the mass range between 1–3 TeV, using the current run2 data with 139 fb^{-1}. Naively rescaling the size of the data to an integrated luminosity of 3 ab^{-1}, assuming the statistical uncertainty dominates, the future sensitivities at the HL-LHC extend to $\mathcal{O}(0.2 - 1$ fb).

The model-independent bounds could be transformed into a useful form, e.g. the total branching fraction of the resonant particle in figure 1, in a wide class of BSM scenarios where the resonant particle production cross sections are the same as (or simply rescaled from) the neutral heavy Higgs production cross sections in 2HDM type-II. If the branching fraction of one's interest is 50%, the heavy Higgs mass up to about 1.3 (2.1) TeV for $m_{e_4} \gtrsim 500$ GeV and $\tan\beta = 10$ (50) can be constrained from the current search results for the $2\ell + E_T^{\text{miss}}$ channel, while the coverage slightly reduces for the $3/4\ell$ channel. The corresponding future coverage at the HL-LHC (for the $2\ell + E_T^{\text{miss}}$) extends to 1.8 and 2.8 TeV for $\tan\beta = 10$ and 50, respectively.

JHEP10(2022)138

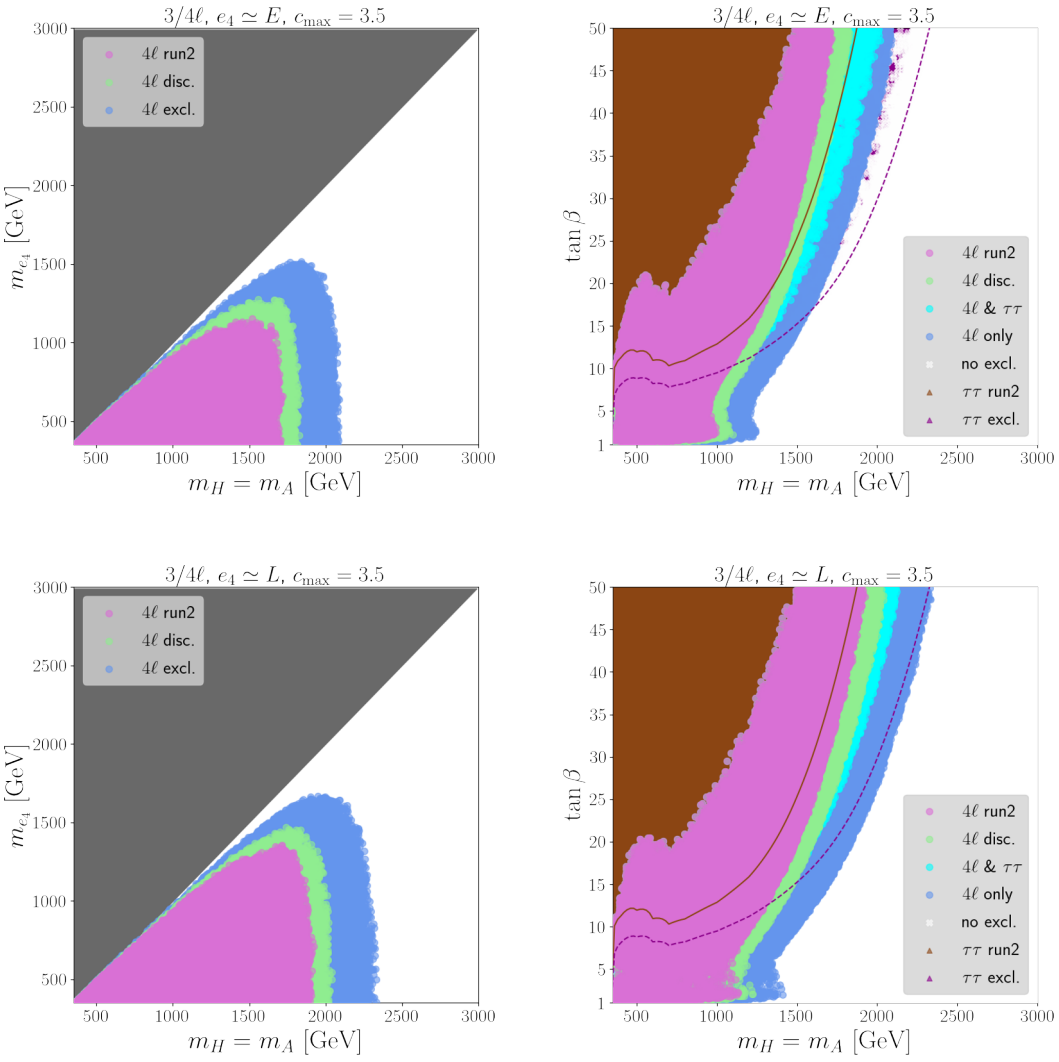

Figure 15. Sensitivities of the $3/4\ell$ search to the light-E (light-L) scenario with $c_{\max} = 3.5$ in the upper (lower) panels. The labels are the same as those in figure 13.

In terms of model-dependent parameters such as $\tan\beta$ and the masses of the new particles, the sensitivities of our leptonic cascade contributing to the $2\ell + E_T^{\text{miss}}$ and $3/4\ell$ channels can be better than what are expected in conventional searches for BSM Higgses such as the nominal $H/A \to \tau\tau$ channel. The current sensitivity covers the region $1 \lesssim \tan\beta \lesssim 10$ up to heavy Higgs masses around 1 TeV, beyond the reach of the conventional searches. The future sensitivities in this region of $\tan\beta$ extend up to $m_{H/A} \lesssim 2.2\,\text{TeV}$ and $m_{e_4} \lesssim 1.5\,\text{TeV}$ at the HL-LHC.

Although not implemented here, we expect that further investigation of an additional lepton resonance from the decay of e_4 would increase the sensitivity of the $3/4\ell$ channel. Therefore, we conclude that searches for our leptonic cascade processes can shed light on probing both an extended Higgs sector and extra matter, and are generally more advantageous than conventional heavy Higgs searches in these scenarios.

JHEP10(2022)138

SF-0J	[100, 105]	[105, 110]	[110, 120]	[120, 140]	[140, 160]	[160, 180]	[180, 220]	[220, 260]	[260, ∞]
ggF-EZ	0.0004	0.0003	0.0009	0.0013	0.0018	0.0015	0.0032	0.0028	0.0255
ggF-EW	0.0004	0.0002	0.0007	0.0012	0.0013	0.0014	0.0028	0.0021	0.0080
ggF-NW	0.0003	0.0003	0.0007	0.0012	0.0013	0.0014	0.0025	0.0024	0.0092
bbH-EZ	0.0006	0.0008	0.0013	0.0033	0.0033	0.0033	0.0065	0.0067	0.0525
bbH-EW	0.0009	0.0007	0.0014	0.0029	0.0025	0.0025	0.0051	0.0041	0.0162
bbH-NW	0.0007	0.0007	0.0014	0.0026	0.0026	0.0028	0.0053	0.0050	0.0184
SF-1J	[100, 105]	[105, 110]	[110, 120]	[120, 140]	[140, 160]	[160, 180]	[180, 220]	[220, 260]	[260, ∞]
ggF-EZ	0.0009	0.0011	0.0022	0.0038	0.0037	0.0042	0.0080	0.0076	0.0657
ggF-EW	0.0010	0.0008	0.0014	0.0029	0.0034	0.0031	0.0061	0.0053	0.0203
ggF-NW	0.0006	0.0008	0.0017	0.0035	0.0032	0.0031	0.0068	0.0063	0.0234
bbH-EZ	0.0010	0.0009	0.0019	0.0045	0.0038	0.0043	0.0081	0.0089	0.0706
bbH-EW	0.0008	0.0010	0.0017	0.0037	0.0030	0.0028	0.0069	0.0057	0.0212
bbH-NW	0.0009	0.0006	0.0013	0.0034	0.0036	0.0035	0.0066	0.0062	0.0243
DF-0J	[100, 105]	[105, 110]	[110, 120]	[120, 140]	[140, 160]	[160, 180]	[180, 220]	[220, 260]	[260, ∞]
ggF-EW	0.0003	0.0003	0.0005	0.0011	0.0011	0.0012	0.0017	0.0019	0.0070
ggF-NW	0.0003	0.0003	0.0005	0.0011	0.0011	0.0010	0.0024	0.0019	0.0085
bbH-EW	0.0005	0.0006	0.0012	0.0020	0.0022	0.0024	0.0045	0.0040	0.0145
bbH-NW	0.0004	0.0005	0.0013	0.0023	0.0022	0.0022	0.0048	0.0042	0.0164
DF-1J	[100, 105]	[105, 110]	[110, 120]	[120, 140]	[140, 160]	[160, 180]	[180, 220]	[220, 260]	[260, ∞]
ggF-EW	0.0007	0.0004	0.0015	0.0024	0.0028	0.0029	0.0051	0.0052	0.0170
ggF-NW	0.0005	0.0004	0.0015	0.0029	0.0027	0.0026	0.0056	0.0048	0.0198
bbH-EW	0.0007	0.0007	0.0016	0.0030	0.0030	0.0025	0.0051	0.0050	0.0182
bbH-NW	0.0007	0.0007	0.0015	0.0031	0.0030	0.0034	0.0057	0.0054	0.0212

Table 3. Efficiencies for the m_{T2} bins in the SRs of the $2\ell + E_T^{\rm miss}$ search from each production processes. The masses are $(m_\Phi, m_{e_4}) = (1500, 750)$ GeV.

We could use the signal with hadronically decaying Z/W boson instead of the leptonic decays, and hence the signal is 0–$2\mu + V_h$, where V_h is the hadronically decaying Z or W. In this case, the signal increases due to the larger branching fractions, but the backgrounds would also increase. This is an interesting possibility but is beyond the scope of this paper.

Lastly, our analysis results can be readily applied to other BSM models where event topologies as in figure 1 are present. Comparing our results to a given reference model, the production cross section of Φ at the LHC and its branching ratios can be simply rescaled. We hence encourage the colleagues in this field to seriously adopt our suggestions in this paper.

Acknowledgments

The authors thank Kyoungchul Kong and Chan Beom Park for useful discussion. The work of R.D. was supported in part by the U.S. Department of Energy under Award No. DE-SC0010120. The work of J.K. is supported in part by the Institute for Basic Science (IBS-R018-D1) and the Grant-in-Aid for Scientific Research from the Ministry of Education, Science, Sports and Culture (MEXT), Japan No. 18K13534. TRIUMF receives federal funding via a contribution agreement with the National Research Council of Canada. S.S. acknowledges support from the National Research Foundation of Korea (NRF-2020R1I1A3072747 and NRF-2022R1A4A5030362).

A Tables of results

In this appendix, the values of our results of the simulations are tabulated. Table 3 shows the efficiencies from the production processes into the m_{T2} bins in the signal regions (SRs) for the $2\ell + E_T^{\rm miss}$ search. The unit for m_{T2} is GeV. The masses of the scalar Φ and vectorlike lepton ℓ_4 are 1500 GeV and 750 GeV, respectively. The efficiencies for the SRs

JHEP10(2022)138

$3/4\ell$	3ℓ-< 50-1Z	3ℓ-> 50-1Z	3ℓ-< 50-0Z	3ℓ-> 50-0Z	4ℓ-< 50-1Z	4ℓ-> 50-1Z	4ℓ-0Z
ggF-EZ	0.0152	0.0128	0.0229	0.0267	0.0582	0.0296	0.0101
bbH-EZ	0.0144	0.0127	0.0225	0.0242	0.0620	0.0292	0.0107

Table 4. Efficiencies for $3/4\ell$ searches. $\lesseqgtr 50$ is for $E_T^{\rm miss}$. $(m_\Phi, m_{e_4}) = (1500, 750)\,\text{GeV}$.

σ [fb]	2ℓ ggF-EZ	2ℓ ggF-EW	2ℓ ggF-NW	2ℓ bbH-EZ	2ℓ bbH-EW	2ℓ bbH-NW	4ℓ ggF-EZ	4ℓ bbH-EZ
current	1.991	3.486	3.078	1.615	2.828	2.505	3.384	3.351
HL-dics.	1.377	1.982	1.737	1.023	1.549	1.363	2.297	2.224
HL-excl.	0.536	0.760	0.665	0.396	0.596	0.524	0.903	0.873

Table 5. Upper bounds on cross section $pp \to \Phi \to \ell_2\ell_4(\to \ell_2 V)$ [fb]. $(m_\Phi, m_{e_4}) = (1500, 750)\,\text{GeV}$.

$\text{Br}_H = 1.0$	2ℓ EZ	2ℓ EW	2ℓ NW	4ℓ EZ
current	1537.288	1399.283	1404.952	1381.412
HL-dics.	1645.134	1551.577	1617.650	1472.274
HL-excl.	1887.796	1798.656	1929.234	1688.689
$\text{Br}_H = 0.5$	2ℓ EZ	2ℓ EW	2ℓ NW	4ℓ EZ
current	1376.797	1239.417	945.943	1236.742
HL-dics.	1479.211	1376.779	1351.959	1330.480
HL-excl.	1709.333	1613.686	1702.713	1523.494

Table 6. Lower bounds on the Higgs mass $m_H = m_A$ in GeV, where Br_H is the branching fraction of the corresponding decay mode of the Higgs boson. $m_{e_4} = 750\,\text{GeV}$, $\tan\beta = 10$.

$\text{Br}_H = 1.0$	2ℓ EZ	2ℓ EW	2ℓ NW	4ℓ EZ
current	2390.634	2226.461	2407.530	2193.706
HL-dics.	2533.524	2428.742	2659.211	2314.561
HL-excl.	2847.526	2733.215	3009.633	2629.996
$\text{Br}_H = 0.5$	2ℓ EZ	2ℓ EW	2ℓ NW	4ℓ EZ
current	2176.036	2034.467	2172.052	1992.152
HL-dics.	2307.396	2207.350	2411.844	2093.795
HL-excl.	2618.456	2508.928	2751.801	2401.660

Table 7. Lower bounds on the Higgs mass $m_H = m_A$ in GeV. where Br_H is the branching fraction of the corresponding decay mode of the Higgs boson. $m_{e_4} = 750\,\text{GeV}$, $\tan\beta = 50$.

in the $3/4\ell$ searches are shown in table 4. Only the SRs with $m_{\rm inv} > 400$ (600) GeV for 3ℓ (4ℓ) shown since the efficiencies are negligible in the other bins for $m_\Phi = 750$ GeV.

The model independent limits on the cross sections are summarized in table 5 using the efficiencies shown tables 3 and 4. The first 6 columns are the limits from $2\ell + E_T^{\rm miss}$ search, while the last 2 columns are the $3/4\ell$ searches. The first, second and third rows are the current 95% C.L. limits, discovery potential with the 3 ab^{-1} data and future exclusion with the 3 ab^{-1} data, respectively.

Tables 6 and 7 are the lower bounds on the Higgs boson mass in the reference model with $\tan\beta = 10$ and 50, respectively. The vectorlike lepton mass is 750 GeV, and the CP-even and CP-odd Higgs boson masses are assumed be the same. In these tables, the

JHEP10(2022)138

Name	Central	Error
G_F	1.1663787×10^{-5}	0.060%
$\mathrm{BR}\,(W \to \mu\nu)$	0.22635	2.4%
$\Gamma\,(Z \to \mathrm{inv})$	0.501464 GeV	0.50%
A_μ	0.142	0.015
A_μ^{FB}	0.0169	0.0013
R_μ	20.784	0.17%
ΔS	-0.01	0.10
ΔT	0.03	0.12
ΔU	0.02	0.11
$R_{\gamma\gamma}$	1.11	0.095

Table 8. Summary of the constraints from the electroweak precision measurements [72] we apply here. The errors with % are relative uncertainties.

upper tables are for the case of $\mathrm{Br}_H = 1.0$ and $\mathrm{Br}_H = 0.5$ for the lower tables, where Br_H is the branching fraction of the leptonic cascade decays to the corresponding decay mode. For instance, $\mathrm{Br}_H = \mathrm{BR}\,(H \to \mu e_4(\to Z\mu))$ for the EZ decay mode. Note that the branching fractions of the Z and W bosons to the SM leptons are not included in Br_H and are assumed to be the SM-like.

B Approximated expressions in the reference model

In this appendix, we summarize analytical formulae of the important EWPOs and decay widths at leading order in:

$$\left| \frac{(\lambda_L, \lambda_E, \lambda, \overline{\lambda}, \kappa_N, \kappa, \overline{\kappa})\, v}{(m_L, m_E, m_N)} \right| \ll 1\,, \tag{B.1}$$

where we define $v \equiv \sqrt{v_u^2 + v_d^2} = 174\,\mathrm{GeV}$ with $v_u = \langle H_u^0 \rangle$ and $v_d = \langle H_d^0 \rangle$. Here the Lagrangian parameters are given in eq. (4.1). Further assuming enough splittings between m_L and m_E (m_N), the lightest charged (neutral) vectorlike lepton e_4 (ν_4) is mostly isodoublet or isosinglet (SM singlet). Detailed approximate expressions of gauge and Yukawa couplings in the mass eigenstate basis are in refs. [30, 71]. Here, we focus on the formulae useful in applying constraints from electroweak precision measurements and several important branching fractions.

B.1 Electroweak precision measurements

The vectorlike leptons in our reference model are constrained by various electroweak precision measurements listed in table 8, which are also discussed in refs. [30, 71]. We calculate these observables at tree-level for the first 6 observables and at the one-loop level for the last 4 observables.

JHEP10(2022)138

The contributions by the vectorlike leptons to the oblique corrections are almost the same as the formulae in ref. [75] given for the vectorlike quarks except the definitions of the following functions:

$$\psi^+(y_a, y_\beta) = \frac{2y_a + 10y_\beta}{3} + \frac{1}{3}\log\frac{y_a}{y_\beta} + \frac{y_a - 1}{6} f(y_a, y_a) + \frac{5y_\beta + 1}{6} f(y_\beta, y_\beta), \tag{B.2}$$

$$\psi^-(y_a, y_\beta) = -\sqrt{y_a y_\beta}\left(4 + \frac{f(y_a, y_a) + f(y_\beta, y_\beta)}{2}\right), \tag{B.3}$$

due to the difference in hypercharges. Here, $y_a := m^2_{\nu_a}/m^2_Z$, $y_\beta := m^2_{e_\beta}/m^2_Z$ $(a, \beta = 1, 2, \cdots, 5)$ and the function $f(y_1, y_2)$ is defined in ref. [75].[11] The ratio $R_{\gamma\gamma} := \Gamma(h \to \gamma\gamma)/\Gamma(h \to \gamma\gamma)_{\rm SM}$ is calculated with the formula shown in ref. [77].

In our reference model, the contributions of vectorlike leptons to the Fermi constant G_F, determined from the muon decay, and $R_\mu := \Gamma(Z \to {\rm had})/\Gamma(Z \to \mu\mu)$ are the most strongly constrained observables in table 8. Hence, we provide the approximate expressions (when eq. (B.1) is valid) of the leading contributions to G_F and R_μ:

$$\frac{\delta G_F}{G_F^{\rm SM}} \sim \frac{v^2/2}{1 + t_\beta^2}\left(\frac{\lambda_E^2}{m_E^2} + t_\beta^2 \frac{\kappa_N^2}{m_N^2}\right) < 6 \times 10^{-4}, \tag{B.4}$$

$$\frac{\delta R_\mu}{R_\mu^{\rm SM}} \sim \frac{4s_W^2}{1 - 4s_W^2 + 8s_W^4}\frac{v_d^2\lambda_L^2}{m_L^2} + \frac{2(1 - 2s_W^2)}{1 - 4s_W^2 + 8s_W^4}\frac{v_d^2\lambda_E^2}{m_E^2} < 1.7 \times 10^{-3}, \tag{B.5}$$

where $t_\beta = \tan\beta$. For $t_\beta \gg 1$, the leading contribution to G_F is κ_N^2/m_N^2 and the other contributions are suppressed by t_β^2. From eq. (B.4), the upper bound on κ_N is estimated as

$$\kappa_N \lesssim \frac{\sqrt{2} m_N}{v s_\beta} \times 6 \times 10^{-4} \sim 1 \times 10^{-3} \times \left(\frac{m_N/s_\beta}{200\ {\rm GeV}}\right). \tag{B.6}$$

Therefore, κ_N should be less than $\mathcal{O}(10^{-3})$ to be consistent with EWPOs. The limits on λ_L and λ_E are weaker by a factor $\tan^2\beta$, and hence $\lambda_{L,E} \sim \mathcal{O}(1)$ is allowed for sufficiently large $\tan\beta$ and vectorlike lepton masses.

B.2 Branching fractions

The partial widths for the heavy netural Higgs decays to the charged leptons, $e_a^+ e_b^-$ $(e_a = \mu, e_4, e_5)$, are given by

$$\Gamma(H \to e_a^+ e_b^-) = \frac{m_H}{16\pi}\beta\left(\frac{m^2_{e_a}}{m_H^2}, \frac{m^2_{e_b}}{m_H^2}\right) \times \left[\left(\left|\left[Y_{\mathbf{e}}^H\right]_{ab}\right|^2 + \left|\left[Y_{\mathbf{e}}^H\right]_{ba}\right|^2\right)\left(1 - \frac{m^2_{e_a}}{m_H^2} - \frac{m^2_{e_b}}{m_H^2}\right) - \frac{4 m_{e_a} m_{e_b}}{m_H^2}{\rm Re}\left(\left[Y_{\mathbf{e}}^H\right]_{ab}\left[Y_{\mathbf{e}}^H\right]_{ba}\right)\right], \tag{B.7}$$

where $\beta(x, y) := \sqrt{1 - 2(y + x) + (y - x)^2}$. Here, $Y_{\mathbf{e}}^H$ is the heavy CP-even Higgs Yukawa matrix of the charged leptons in the mass basis. Those for the CP-odd Higgs boson can be obtained by replacing $H \to A$, and those for the neutrinos are given by replacing $e \to \nu$ and $\mu \to \nu_\mu$.

[11] The doublet-like vectorlike lepton can explain the recent anomaly in the W boson mass [73] if its mass is lighter than 200 GeV and the mixing with the singlet-like state is sizable [76].

JHEP10(2022)138

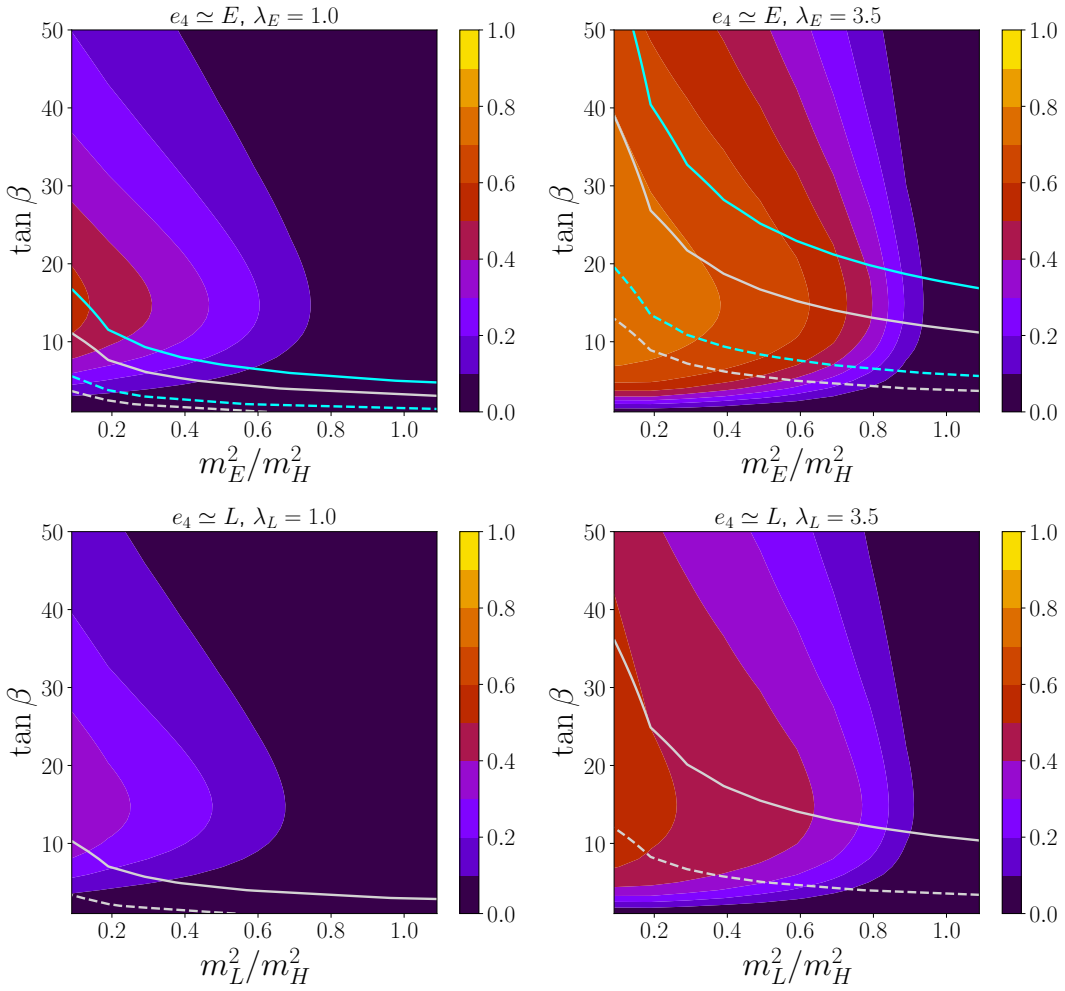

Figure 16. Branching fractions of the leptonic cascade decay, $H \to \mu e_4 \to V\ell_2\mu$, for $m_H = 1$ TeV. G_F (R_μ) is more than 2σ away from the measured value below the cyan (gray) solid line. The EWPO constraints for $m_H = 3$ TeV are shown by the dashed lines.

When e_4 and ν_4 are mostly doublet-like, i.e. $(e_4^-, \nu_4) \sim (L^-, L^0)$, the decay widths to a vectorlike lepton and a SM lepton are approximately given by

$$\Gamma\left(H \to \mu^- L^+\right) \sim \frac{m_H \lambda_L^2 s_\beta^2}{32\pi}\left(1 - \frac{m_L^2}{m_H^2}\right)^2, \tag{B.8}$$

$$\Gamma\left(H \to \nu_\mu L^0\right) \sim \frac{m_H \kappa_N^2 c_\beta^2}{32\pi}\left(1 - \frac{m_L^2}{m_H^2}\right)^2 \left(\frac{\overline{\kappa} v_u}{m_N}\frac{\kappa m_L + \overline{\kappa} m_N}{m_N^2 - m_L^2} v_u\right)^2, \tag{B.9}$$

and for mostly singlet-like leptons, i.e. $e_4^- \sim E$, $\nu_4 \sim N$,

$$\Gamma\left(H \to \mu^- E^+\right) \sim \frac{m_H \lambda_E^2 s_\beta^2}{32\pi}\left(1 - \frac{m_E^2}{m_H^2}\right)^2, \tag{B.10}$$

JHEP10(2022)138

$$\Gamma\left(H \to \nu_\mu N\right) \sim \frac{m_H \kappa_N^2 c_\beta^2}{32\pi}\left(1-\frac{m_N^2}{m_H^2}\right)^2 . \tag{B.11}$$

Here the sub-dominant contributions suppressed by the new Yukawa couplings times $v^2/m_{\rm VLL}^2$, VLL $= E, L, N$, and the SM lepton masses are neglected. Note that $H \to \nu_\mu L^0$ appears only at sub-leading order and vanishes for $\kappa_N = 0$. Thus, the Higgs boson decays mostly to a charged vectorlike lepton and a SM lepton when λ_L (λ_E) is large and $e_4^- \simeq L^-$ (E).

In the numerical analysis, the heavy Higges decay to SM particles, $H \to cc$, bb, tt, $\tau\tau$, $\gamma\gamma$, gg, hh and $A \to cc$, bb, tt, $\tau\tau$, $\gamma\gamma$, gg are calculated using the formulas presented in ref. [1]. We assume the MSSM for the triple Higgs coupling. The decays to gauge bosons, $H \to ZZ$, WW, and $A \to hZ$ vanish in the alignment limit.

The partial decay widths of the charged vectorlike lepton e_4 is given by

$$\begin{aligned}\Gamma\left(e_4 \to h\mu\right) = \frac{m_{e_4}}{64\pi}\beta(x_h, y_\mu)\Bigg[\left(\left|\left[Y_{\mathbf{e}}^h\right]_{\mu e_4}\right|^2 + \left|\left[Y_{\mathbf{e}}^h\right]_{e_4\mu}\right|^2\right)(1+y_\mu-x_h) \\ +4\sqrt{y_\mu}\,\mathrm{Re}\left(\left[Y_{\mathbf{e}}^h\right]_{e_4\mu}\left[Y_{\mathbf{e}}^h\right]_{\mu e_1}\right)\Bigg] ,\end{aligned} \tag{B.12}$$

$$\begin{aligned}\Gamma\left(e_4 \to Z\mu\right) = \frac{m_{e_4}}{32\pi x_Z}\beta(x_Z, y_\mu)\Bigg[\left(\left|\left[g_{e_L}^Z\right]_{\mu e_4}\right|^2 + \left|\left[g_{e_R}^Z\right]_{\mu e_4}\right|^2\right) \\ \times\left\{(1-y_\mu)^2 + x_Z\,(1+y_\mu) - 2x_Z^2\right\} - 3x_Z\sqrt{y_\mu}\,\mathrm{Re}\left(\left[g_{e_L}^Z\right]_{\mu e_4}\left[g_{e_R}^Z\right]_{\mu e_4}\right)\Bigg] ,\end{aligned} \tag{B.13}$$

$$\Gamma\left(e_4 \to W\nu_\mu\right) = \frac{m_{e_4}}{32\pi x_W}\left(\left|\left[g_L^W\right]_{\nu_\mu e_4}\right|^2 + \left|\left[g_R^W\right]_{\nu_\mu e_4}\right|^2\right)(1-x_W)^2\,(1+2x_W) , \tag{B.14}$$

where $Y_{\mathbf{e}}^h$, $g_{e_{L,R}}^Z$ and $g_{L,R}^W$ are the coupling matrices to the SM bosons in the mass basis, see refs. [30, 71] for the details. The mass squared ratios are defined as $y_\mu := m_\mu^2/m_{e_4}^2$ and $x_B := m_B^2/m_{e_4}^2$ with $B = h, Z, W$. Those for the vector-like neutrino ν_4 can be obtained by formally replacing $e \to \nu$ and $[g_{L,R}^W]_{\nu_\mu e_4} \to [g_{L,R}^W]_{\nu_4\mu}$ in the decay to a W boson.

In our analysis, we assume only one of the vectorlike leptons is lighter than the heavy Higgs for simplicity. For the "light-E" scenario, i.e., $e_4 \sim E$, the partial widths are approximately given by

$$\Gamma(e_4 \to h\mu) \sim \frac{c_\beta^2 \lambda_E^2 m_E}{64\pi}(1-x_h)^2 , \tag{B.15}$$

$$\Gamma(e_4 \to Z\mu) \sim \frac{c_\beta^2 \lambda_E^2 m_E}{64\pi}(1-x_Z)^2(1+2x_Z) , \tag{B.16}$$

$$\Gamma(e_4 \to W\nu_\mu) \sim \frac{c_\beta^2 \lambda_E^2 m_E}{32\pi}(1-x_W)^2(1+2x_W) . \tag{B.17}$$

For the "light-L" scenario, i.e., $e_4^- \sim L^-$, the partial decay widths are approximately given by

$$\Gamma(e_4 \to h\mu) \sim \frac{c_\beta^2 \lambda_L^2 m_L}{64\pi}(1-x_h)^2 , \tag{B.18}$$

JHEP10(2022)138

$$\Gamma(e_4 \to Z\mu) \sim \frac{c_\beta^2 \lambda_L^2 m_L}{64\pi}(1-x_Z)^2(1+2x_Z)\,, \tag{B.19}$$

$$\Gamma(e_4 \to W\nu_\mu) \sim \frac{c_\beta^2 \lambda_E^2 m_L}{32\pi}\left(\frac{\overline{\lambda} m_E + \lambda m_L}{m_E^2 - m_L^2} v_d\right)^2 (1-x_W)^2(1+2x_W)\,. \tag{B.20}$$

If ν_4 is mostly isodoublet-like, then we have

$$\Gamma(\nu_4 \to h\nu_\mu) \sim \frac{s_\beta^2 \kappa_N^2 m_L}{64\pi}(1-x_h)^2\left(\frac{\overline{\kappa} v_u}{m_N} + \frac{\kappa m_L + \overline{\kappa} m_N}{m_N^2 - m_L^2} v_u\right)^2\,, \tag{B.21}$$

$$\Gamma(\nu_4 \to Z\nu_\mu) \sim \frac{s_\beta^2 \kappa_N^2 m_L^3}{64\pi m_N^2}(1-x_Z)^2(1+2x_Z)\left(\frac{\overline{\kappa} m_L + \kappa m_N}{m_N^2 - m_L^2} v_u\right)^2\,, \tag{B.22}$$

$$\Gamma(\nu_4 \to W\mu) \sim \frac{c_\beta^2 \lambda_L^2 m_L}{32\pi}(1-x_W)^2(1+2x_W)\,, \tag{B.23}$$

while if it is mostly singlet-like, then

$$\Gamma(\nu_4 \to h\nu_\mu) \sim \frac{s_\beta^2 \kappa_N^2 m_N}{64\pi}(1-x_h)^2\,, \tag{B.24}$$

$$\Gamma(\nu_4 \to Z\nu_\mu) \sim \frac{s_\beta^2 \kappa_N^2 m_N}{64\pi}(1-x_Z)^2(1+2x_Z)\,, \tag{B.25}$$

$$\Gamma(\nu_4 \to W\mu) \sim \frac{s_\beta^2 \kappa_N^2 m_N}{32\pi}(1-x_W)^2(1+2x_W)\left[1+\left(\frac{\lambda_L m_N v_d}{\kappa_N m_L}\frac{\kappa m_L + \overline{\kappa} m_N}{m_N^2 - m_L^2}\right)^2\right]\,. \tag{B.26}$$

In the limit of $\kappa_N \ll \lambda_L, \lambda_E$, the lepton ν_4 can dominantly decay to a W boson.

Figure 16 shows the values of the branching fractions of the leptonic cascade decay $H \to e_4\mu \to V\ell_2\mu$, with $V\ell_2 = Z\mu,\ W\nu_\mu$. In the upper (lower) panels, the hierarchy $m_E < m_H < m_L, m_N$ ($m_L < m_H < m_E, m_N$) is assumed such that $e_4 \simeq E$ (L). The Higgs mass is 1 TeV and the heavier vectorlike lepton masses are set to be 3 TeV. The Yukawa coupling constant λ_E (λ_L) is set to 1.0 or $3.5 \sim \sqrt{4\pi}$ on the left and right panels, respectively, for the case of $e_4 \simeq E$ (L). The other Yukawa coupling constants are set to 10^{-3} for simplicity. In addition, we fix $\kappa_N = 0$ to suppress the contribution to G_F. The regions below the cyan (gray) line is 2σ away from the measured value of G_F (R_μ). G_F provides the stronger constraint for an isosinglet-like e_4, while only that of R_μ provides a constraint for an isodoublet-like e_4 due to the assumption $\kappa_N = 0$. When λ_E (λ_L) $= 1$, the branching fraction can be as large as 50% (40%) for a singlet-like (doublet-like) e_4. If we allow larger coupling constants, BR $(H \to e_4\mu) \sim 1$ is possible, thus, the total branching fraction can be as large as BR $(e_4 \to V\ell)$, i.e., 50% (75%) for the doublet-like (singlet-like) e_4. The decay to the neutral component L^0 vanishes because of $\kappa_N = 0$.

Figure 17 shows the branching fraction $H \to \nu_4\nu_\mu \to W\mu\nu_\mu$ where ν_4 is the SM singlet-like. The constraints from the electroweak precision measurements and the $H \to \tau\tau$ searches are also displayed with the brown and yellow lines, respectively. The value of G_F is more than 2σ away from the measured value to the right of the red lines for $m_N = 250$ (2500) GeV in the left (right) panel. In the left panel, the region above the yellow dash-dot line is

JHEP10(2022)138

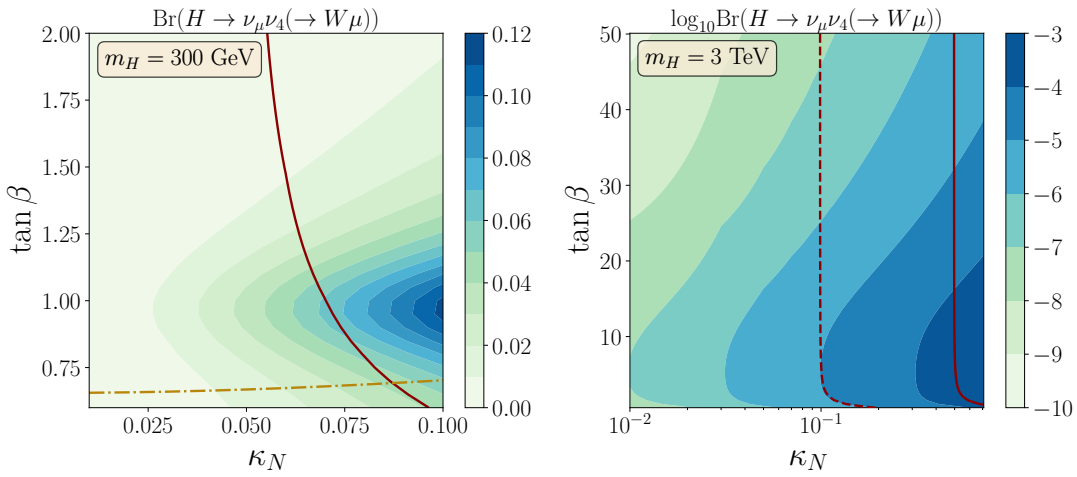

Figure 17. Branching fractions of the leptonic cascade decay via the lightest neutral vectorlike lepton: $H \to \nu_\mu \nu_4 \to V \ell_2 \nu_\mu$ for almost SM singlet-like ν_4. We set $m_H = 300$ (3000) GeV in the left (right) panel. The value of G_F is more than 2σ away from the measured value to the right of the red lines for $m_N = 250$ (2500) GeV in the left (right) panel. In the left panel, the region above the yellow dash-dot line is excluded by the $H \to \tau\tau$ search. The red dashed line in the right panel shows the G_F constraint for $m_N = 500$ GeV.

excluded by the $H \to \tau\tau$ search. The red dashed line in the right panel shows the G_F constraint for $m_N = 500$ GeV. In the left panel, we set $m_H = 300$ GeV $< 2m_t$, where the branching fraction can be as large as 10 %. However, a wide range of parameter space $\tan\beta \gtrsim 0.75$ is already excluded by the recent $H \to \tau\tau$ search. Below the yellow line, the CP-even (CP-odd) Higgs decay is dominated by $H \to hh$ ($A \to gg$) because we assume a MSSM-like Higgs potential. Hence the decay to tau leptons are suppressed. This region can be further excluded by the searches for $H \to hh$ depending on the quartic couplings of Higgs potential [78, 79]. The value of BR $(H \to \nu_4 \nu_\mu)$ is even smaller for larger $\tan\beta$ because the decay widths to bottom quarks and tau leptons are enhanced by $\tan^4\beta$ compared with the decay to the decay mode into ν_4. On the right panel, we assume $m_H = 3$ TeV which is well above the limit from the di-tau decay channel. Even if $m_N = 2.5$ TeV, $\kappa_N \lesssim 0.5$ is required to be consistent with EW precision measurements. The Higgs width is dominated by decays to SM fermions, top quarks for small $\tan\beta$ while bottom quarks for large $\tan\beta$, and BR $(H \to \nu_4 \nu_\mu)$ is at most $\mathcal{O}(10^{-3})$. The values of the branching fraction would be similar (or slightly smaller) in the regions $m_H < 3$ TeV where our analysis has sensitivities and hence we conclude the leptonic process $H \to \nu_4 \nu_\mu \to W\mu\nu_\mu$ would not be constrained in most of our parameter space.

JHEP10(2022)138

References

[1] A. Djouadi, *The Anatomy of electro-weak symmetry breaking. II. The Higgs bosons in the minimal supersymmetric model*, *Phys. Rept.* **459** (2008) 1 [hep-ph/0503173] [INSPIRE].

[2] G.C. Branco, P.M. Ferreira, L. Lavoura, M.N. Rebelo, M. Sher and J.P. Silva, *Theory and phenomenology of two-Higgs-doublet models*, *Phys. Rept.* **516** (2012) 1 [arXiv:1106.0034] [INSPIRE].

[3] S. Dimopoulos and H. Georgi, *Softly Broken Supersymmetry and* SU(5), *Nucl. Phys. B* **193** (1981) 150 [INSPIRE].

[4] H.P. Nilles, *Supersymmetry, Supergravity and Particle Physics*, *Phys. Rept.* **110** (1984) 1 [INSPIRE].

[5] A.R. Zhitnitsky, *On Possible Suppression of the Axion Hadron Interactions (in Russian)*, *Sov. J. Nucl. Phys.* **31** (1980) 260 [INSPIRE].

[6] M. Dine, W. Fischler and M. Srednicki, *A Simple Solution to the Strong CP Problem with a Harmless Axion*, *Phys. Lett. B* **104** (1981) 199 [INSPIRE].

[7] Z. Chacko, H.-S. Goh and R. Harnik, *The Twin Higgs: Natural electroweak breaking from mirror symmetry*, *Phys. Rev. Lett.* **96** (2006) 231802 [hep-ph/0506256] [INSPIRE].

[8] S. Bar-Shalom, M. Geller, S. Nandi and A. Soni, *Two Higgs doublets, a 4th generation and a* 125 *GeV Higgs: A review*, *Adv. High Energy Phys.* **2013** (2013) 672972 [arXiv:1208.3195] [INSPIRE].

[9] R. Dermisek, *Insensitive Unification of Gauge Couplings*, *Phys. Lett. B* **713** (2012) 469 [arXiv:1204.6533] [INSPIRE].

[10] R. Dermisek, *Unification of gauge couplings in the standard model with extra vectorlike families*, *Phys. Rev. D* **87** (2013) 055008 [arXiv:1212.3035] [INSPIRE].

[11] R. Dermisek and N. McGinnis, *Mass scale of vectorlike matter and superpartners from IR fixed point predictions of gauge and top Yukawa couplings*, *Phys. Rev. D* **97** (2018) 055009 [arXiv:1712.03527] [INSPIRE].

[12] R. Dermíšek and N. McGinnis, *Top-bottom-tau Yukawa coupling unification in the MSSM plus one vectorlike family and fermion masses as IR fixed points*, *Phys. Rev. D* **99** (2019) 035033 [arXiv:1810.12474] [INSPIRE].

[13] R. Dermíšek and N. McGinnis, *Seven largest couplings of the standard model as IR fixed points*, *Phys. Rev. Lett.* **122** (2019) 181803 [arXiv:1812.05240] [INSPIRE].

[14] M.J. Dugan, H. Georgi and D.B. Kaplan, *Anatomy of a Composite Higgs Model*, *Nucl. Phys. B* **254** (1985) 299 [INSPIRE].

[15] N. Arkani-Hamed, A.G. Cohen and H. Georgi, *Electroweak symmetry breaking from dimensional deconstruction*, *Phys. Lett. B* **513** (2001) 232 [hep-ph/0105239] [INSPIRE].

[16] J.E. Kim, *Weak Interaction Singlet and Strong CP Invariance*, *Phys. Rev. Lett.* **43** (1979) 103 [INSPIRE].

[17] M.A. Shifman, A.I. Vainshtein and V.I. Zakharov, *Can Confinement Ensure Natural CP Invariance of Strong Interactions?*, *Nucl. Phys. B* **166** (1980) 493 [INSPIRE].

[18] M. Dine and W. Fischler, *A Phenomenological Model of Particle Physics Based on Supersymmetry*, *Phys. Lett. B* **110** (1982) 227 [INSPIRE].

JHEP10(2022)138

[19] C.R. Nappi and B.A. Ovrut, *Supersymmetric Extension of the* SU(3) × SU(2) × U(1) *Model*, *Phys. Lett. B* **113** (1982) 175 [INSPIRE].

[20] L. Álvarez-Gaumé, M. Claudson and M.B. Wise, *Low-Energy Supersymmetry*, *Nucl. Phys. B* **207** (1982) 96 [INSPIRE].

[21] M. Dine and A.E. Nelson, *Dynamical supersymmetry breaking at low-energies*, *Phys. Rev. D* **48** (1993) 1277 [hep-ph/9303230] [INSPIRE].

[22] M. Dine, A.E. Nelson and Y. Shirman, *Low-energy dynamical supersymmetry breaking simplified*, *Phys. Rev. D* **51** (1995) 1362 [hep-ph/9408384] [INSPIRE].

[23] M. Dine, A.E. Nelson, Y. Nir and Y. Shirman, *New tools for low-energy dynamical supersymmetry breaking*, *Phys. Rev. D* **53** (1996) 2658 [hep-ph/9507378] [INSPIRE].

[24] M. Frank and I. Saha, *Muon anomalous magnetic moment in two-Higgs-doublet models with vectorlike leptons*, *Phys. Rev. D* **102** (2020) 115034 [arXiv:2008.11909] [INSPIRE].

[25] E.J. Chun and T. Mondal, *Explaining* $g-2$ *anomalies in two Higgs doublet model with vector-like leptons*, *JHEP* **11** (2020) 077 [arXiv:2009.08314] [INSPIRE].

[26] R. Dermisek, K. Hermanek, N. McGinnis and N. McGinnis, *Highly Enhanced Contributions of Heavy Higgs Bosons and New Leptons to Muon* $g-2$ *and Prospects at Future Colliders*, *Phys. Rev. Lett.* **126** (2021) 191801 [arXiv:2011.11812] [INSPIRE].

[27] R. Dermisek, K. Hermanek and N. McGinnis, *Muon* $g-2$ *in two-Higgs-doublet models with vectorlike leptons*, *Phys. Rev. D* **104** (2021) 055033 [arXiv:2103.05645] [INSPIRE].

[28] R. Dermisek, E. Lunghi and S. Shin, *Two Higgs doublet model with vectorlike leptons and contributions to* $pp \to WW$ *and* $H \to WW$, *JHEP* **02** (2016) 119 [arXiv:1509.04292] [INSPIRE].

[29] R. Dermisek, E. Lunghi and S. Shin, *Contributions of flavor violating couplings of a Higgs boson to* $pp \to WW$, *JHEP* **08** (2015) 126 [arXiv:1503.08829] [INSPIRE].

[30] R. Dermisek, E. Lunghi and S. Shin, *New decay modes of heavy Higgs bosons in a two Higgs doublet model with vectorlike leptons*, *JHEP* **05** (2016) 148 [arXiv:1512.07837] [INSPIRE].

[31] R. Dermisek, E. Lunghi and S. Shin, *New constraints and discovery potential for Higgs to Higgs cascade decays through vectorlike leptons*, *JHEP* **10** (2016) 081 [arXiv:1608.00662] [INSPIRE].

[32] X. Cid Vidal et al., *Report from Working Group 3*: Beyond the Standard Model physics at the HL-LHC and HE-LHC, *CERN Yellow Rep. Monogr.* **7** (2019) 585 [arXiv:1812.07831] [INSPIRE].

[33] R. Dermíšek, E. Lunghi and S. Shin, *Hunting for Vectorlike Quarks*, *JHEP* **04** (2019) 019 [*Erratum ibid.* **10** (2020) 058] [arXiv:1901.03709] [INSPIRE].

[34] R. Dermisek, E. Lunghi and S. Shin, *Cascade decays of heavy Higgs bosons through vectorlike quarks in two Higgs doublet models*, *JHEP* **03** (2020) 029 [arXiv:1907.07188] [INSPIRE].

[35] R. Dermisek, E. Lunghi, N. McGinnis and S. Shin, *Signals with six bottom quarks for charged and neutral Higgs bosons*, *JHEP* **07** (2020) 241 [arXiv:2005.07222] [INSPIRE].

[36] R. Dermisek, J. Kawamura, E. Lunghi, N. McGinnis and S. Shin, *Combined signatures of heavy Higgses and vectorlike fermions at the HL-LHC*, in *2022 Snowmass Summer Study*, (2022) [arXiv:2203.03852] [INSPIRE].

[37] J. Ellis, *TikZ-Feynman: Feynman diagrams with TikZ*, *Comput. Phys. Commun.* **210** (2017) 103 [arXiv:1601.05437] [INSPIRE].

JHEP10(2022)138

[38] M. Dohse, *TikZ-FeynHand: Basic User Guide*, arXiv:1802.00689 [INSPIRE].

[39] ATLAS collaboration, *Search for electroweak production of charginos and sleptons decaying into final states with two leptons and missing transverse momentum in $\sqrt{s} = 13$ TeV pp collisions using the ATLAS detector*, *Eur. Phys. J. C* **80** (2020) 123 [arXiv:1908.08215] [INSPIRE].

[40] ATLAS collaboration, *Search for new phenomena in three- or four-lepton events in pp collisions at $\sqrt{s} = 13$ TeV with the ATLAS detector*, *Phys. Lett. B* **824** (2022) 136832 [arXiv:2107.00404] [INSPIRE].

[41] R. Dermisek, J.P. Hall, E. Lunghi and S. Shin, *Limits on Vectorlike Leptons from Searches for Anomalous Production of Multi-Lepton Events*, *JHEP* **12** (2014) 013 [arXiv:1408.3123] [INSPIRE].

[42] ATLAS collaboration, *Searches for vector-like quarks with the ATLAS detector at the LHC*, *PoS* **EPS-HEP2015** (2015) 152 [INSPIRE].

[43] B. Allanach, F.S. Queiroz, A. Strumia and S. Sun, *Z' models for the LHCb and $g-2$ muon anomalies*, *Phys. Rev. D* **93** (2016) 055045 [*Erratum ibid.* **95** (2017) 119902] [arXiv:1511.07447] [INSPIRE].

[44] J. Kawamura, S. Raby and A. Trautner, *Complete vectorlike fourth family and new U(1)′ for muon anomalies*, *Phys. Rev. D* **100** (2019) 055030 [arXiv:1906.11297] [INSPIRE].

[45] J. Kawamura, S. Raby and A. Trautner, *Complete vectorlike fourth family with U(1)′: A global analysis*, *Phys. Rev. D* **101** (2020) 035026 [arXiv:1911.11075] [INSPIRE].

[46] J. Kawamura and S. Raby, *Signal of four muons or more from a vector-like lepton decaying to a muon-philic Z' boson at the LHC*, *Phys. Rev. D* **104** (2021) 035007 [arXiv:2104.04461] [INSPIRE].

[47] R. Dermisek, J.P. Hall, E. Lunghi and S. Shin, *A New Avenue to Charged Higgs Discovery in Multi-Higgs Models*, *JHEP* **04** (2014) 140 [arXiv:1311.7208] [INSPIRE].

[48] J.F. Gunion, H.E. Haber, G.L. Kane and S. Dawson, *The Higgs Hunter's Guide*, *Front. Phys.* **80** (2000) 1 [INSPIRE].

[49] ATLAS, CMS, LHC Higgs Combination Group collaboration, *Procedure for the LHC Higgs boson search combination in Summer 2011*, CMS-NOTE-2011-005.

[50] G. Cowan, K. Cranmer, E. Gross and O. Vitells, *Asymptotic formulae for likelihood-based tests of new physics*, *Eur. Phys. J. C* **71** (2011) 1554 [*Erratum ibid.* **73** (2013) 2501] [arXiv:1007.1727] [INSPIRE].

[51] C.G. Lester and B. Nachman, *Bisection-based asymmetric M_{T2} computation: a higher precision calculator than existing symmetric methods*, *JHEP* **03** (2015) 100 [arXiv:1411.4312] [INSPIRE].

[52] J. Alwall, R. Frederix, S. Frixione, V. Hirschi, F. Maltoni, O. Mattelaer et al., *The automated computation of tree-level and next-to-leading order differential cross sections, and their matching to parton shower simulations*, *JHEP* **07** (2014) 079 [arXiv:1405.0301] [INSPIRE].

[53] C. Degrande, C. Duhr, B. Fuks, D. Grellscheid, O. Mattelaer and T. Reiter, *UFO — The Universal FeynRules Output*, *Comput. Phys. Commun.* **183** (2012) 1201 [arXiv:1108.2040] [INSPIRE].

JHEP10(2022)138

[54] A. Alloul, N.D. Christensen, C. Degrande, C. Duhr and B. Fuks, *FeynRules 2.0 — A complete toolbox for tree-level phenomenology*, *Comput. Phys. Commun.* **185** (2014) 2250 [arXiv:1310.1921] [INSPIRE].

[55] N.D. Christensen and C. Duhr, *FeynRules — Feynman rules made easy*, *Comput. Phys. Commun.* **180** (2009) 1614 [arXiv:0806.4194] [INSPIRE].

[56] P. Artoisenet, R. Frederix, O. Mattelaer and R. Rietkerk, *Automatic spin-entangled decays of heavy resonances in Monte Carlo simulations*, *JHEP* **03** (2013) 015 [arXiv:1212.3460] [INSPIRE].

[57] T. Sjöstrand, S. Mrenna and P.Z. Skands, *A Brief Introduction to PYTHIA 8.1*, *Comput. Phys. Commun.* **178** (2008) 852 [arXiv:0710.3820] [INSPIRE].

[58] DELPHES 3 collaboration, *DELPHES 3, A modular framework for fast simulation of a generic collider experiment*, *JHEP* **02** (2014) 057 [arXiv:1307.6346] [INSPIRE].

[59] M. Cacciari, G.P. Salam and G. Soyez, *The anti-k_t jet clustering algorithm*, *JHEP* **04** (2008) 063 [arXiv:0802.1189] [INSPIRE].

[60] M. Cacciari, G.P. Salam and G. Soyez, *FastJet User Manual*, *Eur. Phys. J. C* **72** (2012) 1896 [arXiv:1111.6097] [INSPIRE].

[61] F. Caravaglios, M.L. Mangano, M. Moretti and R. Pittau, *A New approach to multijet calculations in hadron collisions*, *Nucl. Phys. B* **539** (1999) 215 [hep-ph/9807570] [INSPIRE].

[62] J.F. Gunion and H.E. Haber, *The CP conserving two Higgs doublet model: The Approach to the decoupling limit*, *Phys. Rev. D* **67** (2003) 075019 [hep-ph/0207010] [INSPIRE].

[63] N. Craig, J. Galloway and S. Thomas, *Searching for Signs of the Second Higgs Doublet*, arXiv:1305.2424 [INSPIRE].

[64] M. Carena, I. Low, N.R. Shah and C.E.M. Wagner, *Impersonating the Standard Model Higgs Boson: Alignment without Decoupling*, *JHEP* **04** (2014) 015 [arXiv:1310.2248] [INSPIRE].

[65] H.E. Haber, *The Higgs data and the Decoupling Limit*, in *1st Toyama International Workshop on Higgs as a Probe of New Physics 2013*, Toyama Japan, February 13–16 2013 [arXiv:1401.0152] [INSPIRE].

[66] CMS collaboration, *Search for additional neutral MSSM Higgs bosons in the $\tau\tau$ final state in proton-proton collisions at $\sqrt{s} = 13$ TeV*, *JHEP* **09** (2018) 007 [arXiv:1803.06553] [INSPIRE].

[67] ATLAS collaboration, *Search for heavy Higgs bosons decaying into two tau leptons with the ATLAS detector using pp collisions at $\sqrt{s} = 13$ TeV*, *Phys. Rev. Lett.* **125** (2020) 051801 [arXiv:2002.12223] [INSPIRE].

[68] ATLAS collaboration, *hMSSM summary plots from direct and indirect searches*, ATL-PHYS-PUB-2020-006.

[69] R.V. Harlander, S. Liebler and H. Mantler, *SusHi: A program for the calculation of Higgs production in gluon fusion and bottom-quark annihilation in the Standard Model and the MSSM*, *Comput. Phys. Commun.* **184** (2013) 1605 [arXiv:1212.3249] [INSPIRE].

[70] R.V. Harlander, S. Liebler and H. Mantler, *SusHi Bento: Beyond NNLO and the heavy-top limit*, *Comput. Phys. Commun.* **212** (2017) 239 [arXiv:1605.03190] [INSPIRE].

[71] R. Dermisek and A. Raval, *Explanation of the Muon $g-2$ Anomaly with Vectorlike Leptons and its Implications for Higgs Decays*, *Phys. Rev. D* **88** (2013) 013017 [arXiv:1305.3522] [INSPIRE].

JHEP10(2022)138

[72] Particle Data Group collaboration, *Review of Particle Physics*, *PTEP* **2020** (2020) 083C01 [INSPIRE].

[73] CDF collaboration, *High-precision measurement of the W boson mass with the CDF II detector*, *Science* **376** (2022) 170 [INSPIRE].

[74] ATLAS collaboration, *Search for type-III seesaw heavy leptons in dilepton final states in pp collisions at* $\sqrt{s} = 13$ *TeV with the ATLAS detector*, *Eur. Phys. J. C* **81** (2021) 218 [arXiv:2008.07949] [INSPIRE].

[75] L. Lavoura and J.P. Silva, *The Oblique corrections from vector — like singlet and doublet quarks*, *Phys. Rev. D* **47** (1993) 2046 [INSPIRE].

[76] J. Kawamura, S. Okawa and Y. Omura, *W boson mass and muon* $g-2$ *in a lepton portal dark matter model*, *Phys. Rev. D* **106** (2022) 015005 [arXiv:2204.07022] [INSPIRE].

[77] A. Djouadi, *The Anatomy of electro-weak symmetry breaking. I: The Higgs boson in the standard model*, *Phys. Rept.* **457** (2008) 1 [hep-ph/0503172] [INSPIRE].

[78] CMS collaboration, *Search for Higgs boson pair production in events with two bottom quarks and two tau leptons in proton-proton collisions at* $\sqrt{s} = 13\,TeV$, *Phys. Lett. B* **778** (2018) 101 [arXiv:1707.02909] [INSPIRE].

[79] ATLAS collaboration, *Search for Higgs boson pair production in the two bottom quarks plus two photons final state in pp collisions at* $\sqrt{s} = 13$ *TeV with the ATLAS detector*, *Phys. Rev. D* **106** (2022) 052001 [arXiv:2112.11876] [INSPIRE].

JHEP10(2022)138